Title	Structure Control and Characterization of Nanoporous Materials Prepared by Mechanical Method
Author(s)	連, 増文
Citation	大阪大学, 2018, 博士論文
Version Type	VoR
URL	https://doi.org/10.18910/69572
rights	
Note	

Doctoral Dissertation

Structure Control and Characterization of Nanoporous Materials Prepared by Mechanical Method

Tseng-Wen Lian

January, 2018

Division of Materials and Manufacturing Science

Graduate School of Engineering,

Osaka University

Contents

Chapter 1

General Introduction

1.1 Introduction

Recently, accompanying with the rapid industrial growth, an extraordinary amount of greenhouse gas emission has been released into the atmosphere. The emission is mainly due to the carbon oxides generated from burning fuels, such as CO_2 gas [1]. Well known as the global warming, the increasing of global surface temperature hence occurred and its tendency dramatically increased during late years [2]. Nowadays, the global warming has becoming a worldwide problem. Furthermore, the problems along with industrial growth and energy usage are not only the global warming but environmental issues such as heat energy pollution, acid precipitation, ozone depletion, and forest destruction. Especially, the issue of waste heat energy generated from industrial furnaces, incinerators, factories, buildings, and houses were receiving great attentions, by reason of their strong relation to the energy-saving.

Therefore, how to reduce the amount of CO_2 emission and waste heat energies more efficiently is of very important environmental subject facing the scientific and technology field today. New technologies for promoting the efficiency of using energy resources will become more and more important. The development of high performance thermal insulation materials is one of the keys to solve these problems. Because the thermal insulations are widely used in engineering fields such as electric power industry, nuclear plant, and space technology. So far, people have tried to make various kinds of thermal insulations. But the manufacturing processes are usually complicated. In particular, there are needs for economic and green methods to produce these materials efficiently. In this consideration, porous ceramics play an important role as the promising materials in thermal insulation field [3-5].

1.2 Features of ceramic materials with porous and nanostructure

Commonly, materials with designed porosity show special features and properties. It is usually difficult to be achieved by the conventional dense process. For such reason, ceramic materials with porous structure are widely used in engineering field nowadays. Generally the porous ceramics have features of high thermal stability for oxidation, high chemical stability, low thermal conductivity, high surface area, low density, and low dielectric constant [6]. The applications of porous ceramics include various advanced materials such as filter, substrate, bio-material, electrolyte and thermal barrier coating. However, the method to fabricate porous ceramics is still much concerned issues [7]. General method to fabricate such materials is gel-casting [8]. But, controlling the portion of solid loading in slurry, long processing time, and product's strength are still problems in using gel-casting method. Therefore, finding a better way to fabricate the porous ceramics is an important issue.

Recently, advanced process for precise controlling of porous materials with nanostructure is receiving the attentions as a key technology for developing the new materials [9]. As well known, pore morphology and pore size distribution can have effect on resultant material's properties. These features are highly influenced by the processing method used in preparing the porous ceramics. By applying advanced process, composition and microstructure of nanoporous materials can be tailored. There are various applications as follows: drug delivery systems [10], solid oxide fuel cell [11], electrode of a lithium ion battery [12-14], and high performance thermal insulation materials [15-17]. In this study the thermal insulation materials are mainly discussed.

1.3 Nanoporous ceramics for advanced thermal insulation materials

1.3.1 Research background and problems

As well known, the development of high performance thermal insulation materials is one of the keys to resolve the energy issue and environmental problem. In general, excellent thermal insulation materials are porous structure and represent very low value of thermal conductivity. From previous papers, it is reported that the supercritically dried silica aerogels is a very promising material [18,19]. It shows extremely low thermal conductivity, owing to its nanoporous structure. However, there are still several problems when in the use of silica aerogels to thermal insulation field. The compact board made of silica aerogels is very fragile. Besides, its thermal insulation ability will be lost while operating in high temperature range [18].

On the other hand, fumed silica is gathering great attention as in advanced materials recently. In previous study, D. R. Smith et al [20,21] had developed the compact made of fumed silica as the better candidate for high performance thermal insulation material. It was produced as a board of bonded composite particles made of fumed silica powder, ceramic fibers, and opacifiers [20,21]. The thermal conductivity of the fumed silica compact can be close to that of silica aerogels [18,19]. It is attributed to the high porosity and nanoporous structure decreasing the thermal conductivity of solid part and that of gas part effectively in the compact [20,21]. Despite the fumed silica compact shows highly efficient thermal insulation ability, the mechanical reliability of the compact is still low and is needed to be handled with great care [20,21]. For the improvement of the mechanical reliability, a large amount of ceramic fibers addition is one of a practice ways. Nevertheless, such addition may result in higher solid conduction of heat transfer, as the number of contact points between fibers in the compact increased.

1.3.2 Nanoporous structure controlling method in this study

(1) Introduction of mechanical processing method

Previous study developed a new mechanical processing method to prepare fiber reinforced porous fumed silica compact [16]. The BET specific surface area of the fumed silica powder was 300 m^2/g, which corresponds to an average particle diameter of about 10 nm. The powder had a three-dimensional nanoscale chain-like aggregated structure with the size of several tens nanometer [16]. Fig. 1.1 shows the schematic illustration of the dry processing method for the fabrication of the compact. The method includes the following three stages: (i) mixing of raw materials (fumed silica nanoparticles, glass fibers, and opacifiers), (ii) mechanical milling to coat glass fiber with fumed silica layer, and (iii) dry pressing of the processed composite powder to produce the compact.

In stage (i), glass fibers were added as reinforcing filler to the compact. In addition, the opacifier particles of SiC were added for controlling the radiation heat transfer of the compact at high temperature [16]. In stage (ii), a horizontal axis type shearing mixer was used for the powder treatment. After mechanical processing of starting powder mixtures, silica nanoparticles were coated on the surface of glass fibers with forming nanoporous structure [15,16], as illustrated in Fig. 1.1. By such processing method, the silica/fiber composite particles were obtained without collapse of fumed silica's nanoscale pores. This is mainly attributed to the appropriate mechanical treatment of metal oxide powders; as a result, it can produce the core/shell type composite particles, without using any binders in dry process [22,23]. In stage (iii), the processed powders were compacted to form the shape of board [15]. Then, the compact board with nanoporous structure was obtained.

The resulted fiber reinforced porous silica compact can be used as an advanced thermal insulation material. It shows efficient thermal insulation ability and enough mechanical strength [16]. This method does not include the steps such as dispersing nanoparticles in a solvent and drying of the solvent [9]. In addition to the intrinsic high surface reactivity of nanoparticles, the chemical bonding is achieved through the enhanced particle surface activation induced by mechanical energy in process. It means the processing method is very effective in manufacturing. With using this feature, desired composite particles can be successfully fabricated. It is considered that this method is a promising approach for producing other advanced nanoporous composite materials.

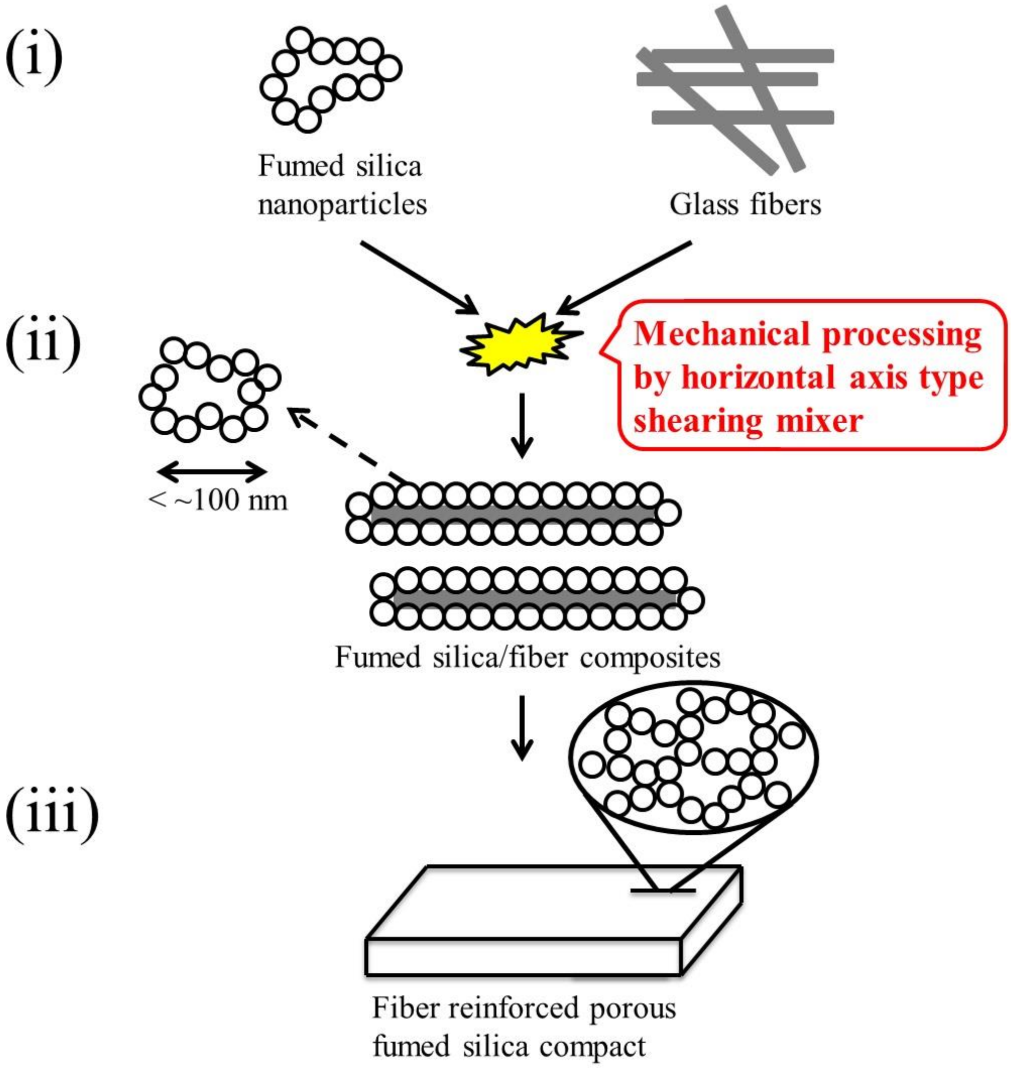

Fig. 1.1 Schematic illustration of the mechanical processing method for the fabrication of the compact with nanoporous structure.

(2) Introduction of mechanical processing apparatus

Figure 1.2 shows the schematic image of the horizontal axis type shearing mixer conducted in mechanical processing. The apparatus mainly consist of 12 blades on a rotary rod, chamber, and motor. The space between the blade and inner side of chamber is 1 mm. The clearance between the rotating rotor and chamber is 3 mm [22]. The blades, rotary rod and chamber are made of SUS 304. During the rotor rotating, powder mixtures are compressed into the clearance and receive various kinds of mechanical stresses, such as compressive and shear stresses, without any media ball or solvent [16,17].

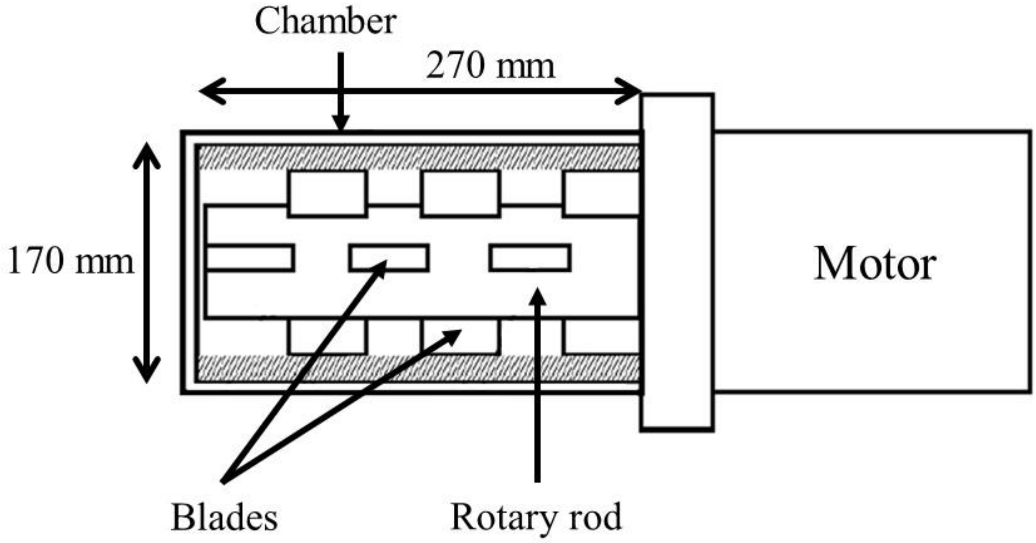

Fig. 1.2 Schematic image of the horizontal axis type shearing mixer conducted in mechanical processing.

(3) Thermal insulation mechanism referred to nanoporous structure

From previous study [16,17], the thickness of the coated fumed silica layer on glass fiber (with 10 μm diameter) was around 2 μm, and the pore size of this porous layer was around 100 nm, observed by microscopic examination. Also, the opacifier particles SiC coated with fumed silica were observed [16]. The results indicated the direct contacts between fiber-fiber, fiber-other particle and SiC-other particle in the compact were prevented by the existence of the coated nanoporous silica layer. And since fumed silica particles were fixed on their surface, the segregation of particles rarely happened during the board forming process. Thus highly uniform dispersion of fibers and SiC in the compact was achieved. As a result, the solid conduction of heat transfer did not increase through the particle contacts at high solid loading amount of fibers and SiC. In addition, as the size of nanoscale pores was near the mean free path of the air molecule (around 70 nm under ambient pressure, and room temperature), the heat transfer of solid and gas parts in the compact were restricted effectively. Combining the above-mentioned effects, the nanoporous compact with extremely low value of thermal conductivity was achieved in this method [16].

1.3.3 Features of fabricated nanoporous compact for thermal insulation

In previous study [16,17,24,25], the ceramic nanoparticles/ceramic fiber compacts were successfully prepared by using the mechanical processing method mentioned in 1.3.2. The ceramic nanoparticles such as hydrophilic fumed silica were used. The produced compacts showed the characteristics of high porosity, light weight, very low thermal conductivity and enough machinability. Fig. 1.3 shows the thermal conductivity of the compacts made by this method and that of the commercial thermal insulation materials in wide temperature range [24,25]. The thermal conductivities of commercial materials such as rock wool, calcium silicate board, and alumina fiber board increase with increasing the measuring temperature obviously. On the other hand, the fabricated nanoporous compact keeps the very low thermal conductivity value around 0.03 W/m·K until 700 °C.

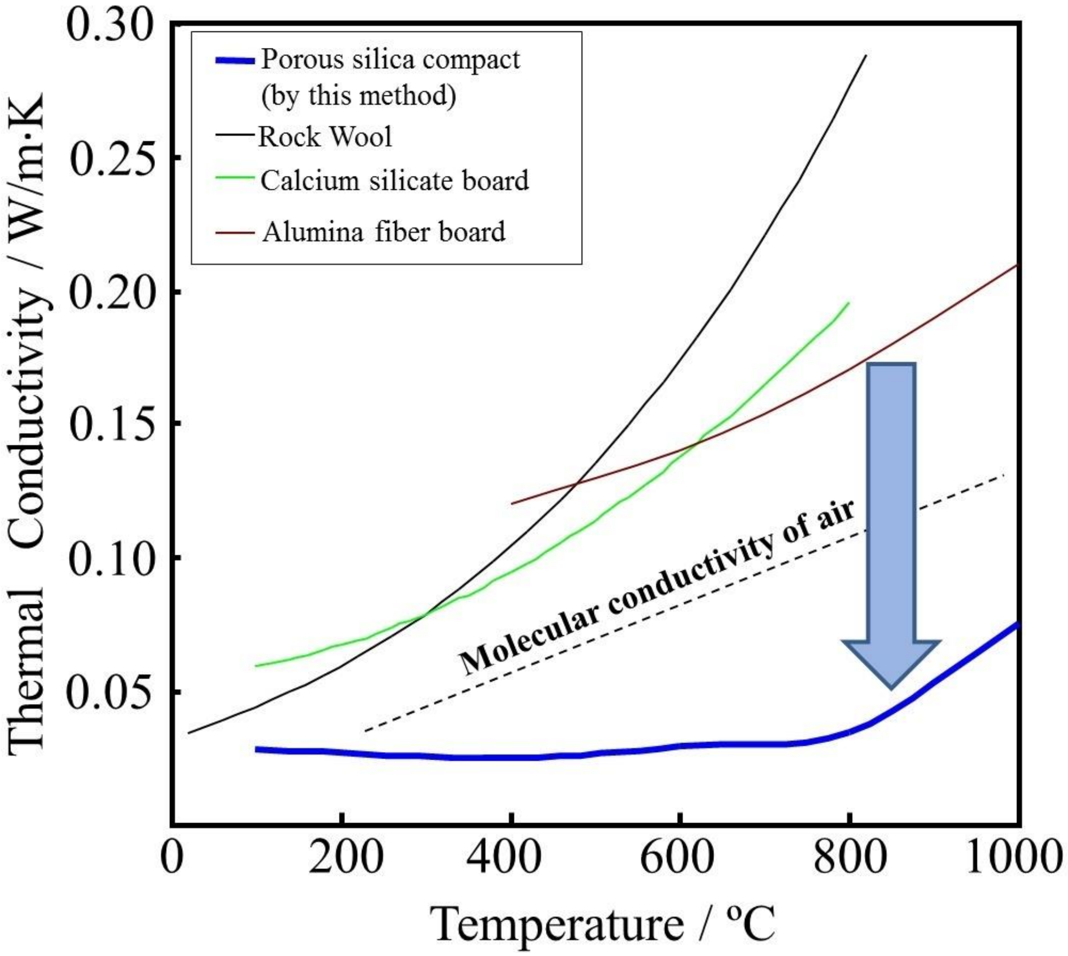

Fig. 1.3 Thermal conductivity of nanoporous compact made by mechanical processing method and that of the commercial thermal insulation materials [24].

1.3.4 Selection of the starting materials

The target nanoporous compact for advanced thermal insulation should be produced as a board of bonded composite particles, mainly made of ceramic nanoparticles, ceramic fibers, and opacifiers. While in selecting the starting materials, following approaches are considered. In selecting ceramic powders, silica is very promising due to its low cost and widely used in engineering field. Thus, the fumed silica nanoparticle is mainly considered in this study. In manufacturing, fumed silica is produced by the vapor phase hydrolysis process of silicon tetrachloride in hydrogen oxide flame [26]. By the manufacturing process, fumed silica powder used in this study shows an average particle diameter of around 10 nm. And its primary particles collide are aggregated together to build up a three-dimensional nanoscale chain-like (dendrite) structure with having pores of several tens nanometer [16,17].

As well known in powder technology, the particle properties such as species of particle, particle size, and surface characteristics play an important role in developing the compact made of composite particles. Therefore, in addition to the above mentioned hydrophilic fumed silica, the surface type of hydrophobic one is also used to investigate the effects on the resultant compact board in this study. Also, the fumed alumina powder is selected to prepare the thermal insulation board for high temperature use.

To improve the mechanical strength of the compact board, the ceramic fibers are added. Ceramics fibers of glass fibers and alumina fiber were tried. And for controlling its thermal conductivity at high temperature, the SiC powders were added to decrease the radiation heat transfer of the compact.

1.3.5 Estimated formula of thermal conductivity in nanoporous materials

The thermal conductivity and the thermal diffusivity are sensitive to the structure of materials. In previous research, estimated formula of thermal conductivity of a compact consisted of nanoporous structure, under atmosphere condition, was proposed by Ohmura et al [27,28]. The equation is shown as below:

$$\lambda = A\rho + B/\rho\ \mathrm{T}^3 + \lambda_g \tag{1.1}$$

where λ is the thermal conductivity, ρ is the apparent density, T is the absolute temperature, λ_g is the thermal conductivity of gas, A is the coefficient of solid part of thermal conductivity, and B is the coefficient of radiation part, respectively. In the method, in addition to the thermal conductivities under atmosphere, that under vacuum is measured. The thermal conductivity under vacuum condition, λ_v, is proposed as the following equation:

$$\lambda_v = A\rho + B/\rho\ \mathrm{T}^3 \tag{1.2}$$

The equation supposed that the thermal conductivity of gas can be neglected under vacuum condition. Thus, from the difference between thermal conductivities under atmosphere and vacuum, the thermal conductivity devoted by the gas in the compact, λ_g, is determined. The coefficient A and B are also determined from the result of experiment. In the analysis, relation between third power of absolute temperature and thermal conductivity under vacuum is plotted. The intercept of graph is given as $A\rho$ and the slope is given as B/ρ in the relationship. Calculating with the known density, the coefficient of A and B is then experimentally obtained.

The estimated formula assumes that the thermal conductivity of a nanoporous thermal insulation material is the sum of solid part (referred to the contacts between solid particles in the material), radiation part, and gas part of thermal conductivity. The terms of $A\rho$, $B/\rho\ T^3$, and λ_g represent the solid part, radiation part, and gas part of thermal conductivity, respectively. In the equation, the solid part does not depend on the temperature is supposed. It is because the thermal insulation materials generally have high porosity structure (low solid content), and hence the heat conduction by solids in material is very small. In the equation, the solid part of thermal conductivity, $A\rho$, is direct proportion to the apparent density. The reason is because the solid part of a material will increase with increasing the apparent density, and will result in increasing the contact points between solids; thus leading to the increase of thermal conductivity. In discussing the term of radiation part, the following reason is concerned. The effect of radiation shielding ability increases with increasing the apparent density. It results in the decrease of thermal conductivity of radiation in materials. Therefore, the radiation part in the equation, $B/\rho\ T^3$, is reciprocal proportion to the apparent density.

1.4 Measuring methods of thermal and mechanical properties for nanoporous materials

1.4.1 Introduction of measuring methods of thermal conductivity and thermal diffusivity

Commonly, excellent thermal insulation materials are porous structure and have very low thermal conductivity. For their further development, to determine the thermal properties of them is becoming an important issue. One of the reasons is that measuring the thermal conductivity more precisely during the developing stage referred to understanding of the thermal insulation ability well; and it is helpful to find the relation between the thermal conductivity and other parameters such as operating temperature and apparent density. In addition, for those people need to use the thermal insulations, the precise thermal conductivity parameter helps their thermal design: such as decreasing the setting space, resource, cost, and saving the energy of installation. However, to determine the thermal conductivity of porous materials with very low heat conduction is a challenging task.

In general, there are two ways to measure the thermal conductivity: steady-state method and transient method [29-33]. Steady-state method [29,30] gives a thermal gradient to the test specimen, and measures the thermal conductivity directly. The guarded hot plate (GHP) method and heat flow meter (HMF) method are representative methods in steady-state method. Especially, the GHP method is also called absolute method and popularly used in standard measuring. Also, this method is frequently used to measure thermal insulation material with very low thermal conductivity (about 0 ~ 2 W/m·K). However, the method has the demerit which needs relatively large specimen (300 mm × 300 mm × 20 mm) and long measuring times (1/2 day ~ 1 day) [29,30]. In addition, the GHP method is difficult to measure the thermal conductivity at higher temperature ranges (>250 °C).

On the other hand, transient method provides transitional thermal flow to the specimen, and determines the thermal conductive properties from the response of the temperature change [31-33]. For instance, the cyclic heat method, laser flash method, 3ω-method, thermoreflectance method, and hot wire method are the representative ones belonging to transient method. Generally, the transient methods only determine the thermal diffusivity α during measuring. The data of specific heat capacity C_p and density ρ are needed for calculating the thermal conductivity λ. The density ρ can be determined from calculating the dimensions and weights of the materials. Also, the specific heat capacity C_p can be obtained from experiment. With knowing the data, the thermal conductivity λ is determined by the equation as below [34]:

$$\lambda = \rho \cdot \alpha \cdot \mathrm{C_p} \tag{1.3}$$

Among above transient methods, unlike to others, the hot wire method can measure the thermal conductivity directly. Thus the method is usually used.

Figure 1.4 shows the applicable ranges of mentioned representative measuring methods of thermal conductivity and thermal diffusivity. The X-axis and Y-axis in figure indicate the applying heat diffusion length and measuring temperature range, respectively. The heat diffusion length is a value corresponding to the size of measured specimen. For measuring the specimen size of thin film, the 3ω-method and thermoreflectance method are commonly used. For the size of μm ~ mm range, the cyclic heat method is used. For the size of mm order, the laser flash method is used. In general, the steady-state method is used to measure the specimen size of cm ~ m range, such as bulk, thermal insulations, and building materials. In contrast, the transient method is used to measure the specimen with relatively small size. The details of several representative thermal conductivity and thermal diffusivity measuring methods referred to this study are introduced in this section.

Table 1.1 shows the comparison of several representative measuring methods of thermal conductivity and thermal diffusivity. Each method’s classes (steady-state method or transient method) and merit/demerit are listed in the table.

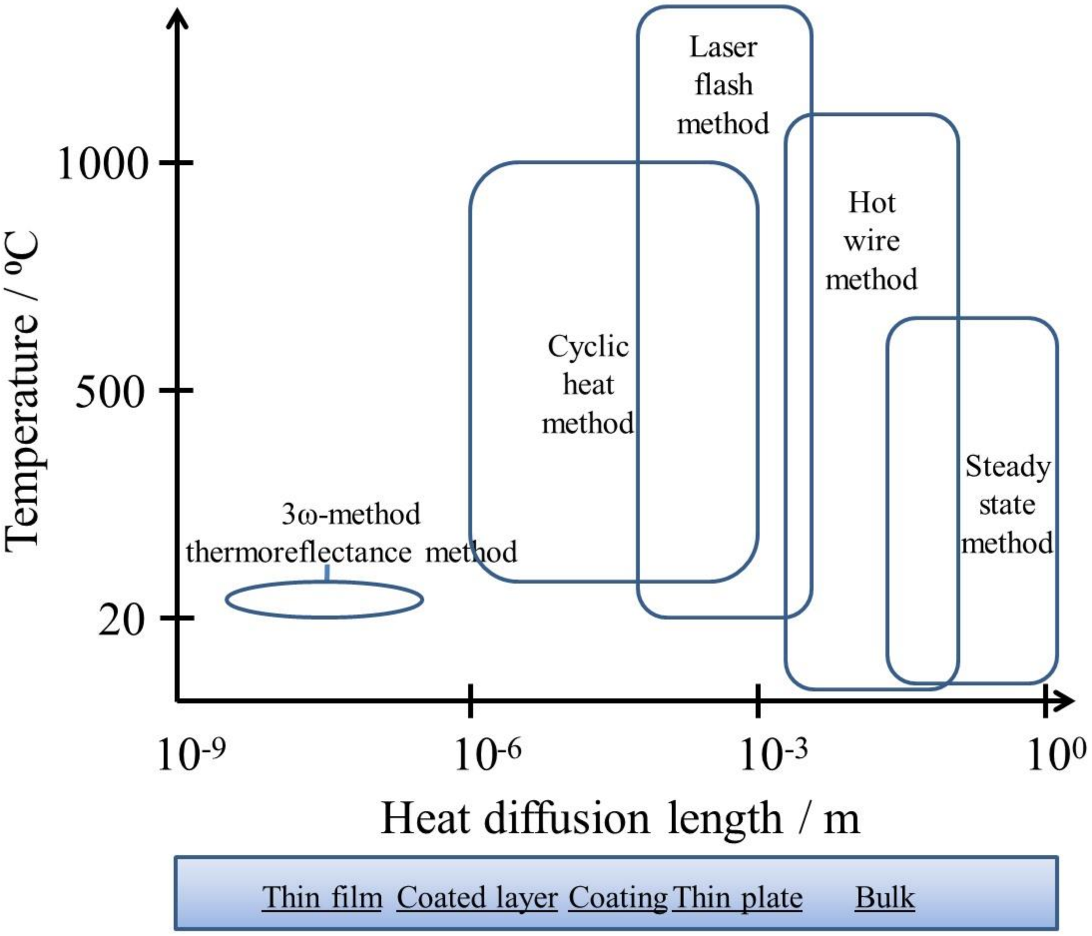

Fig. 1.4 Applicable measuring ranges of representative methods of thermal conductivity and thermal diffusivity measurement.

Table 1.1 Comparison of thermal property measurement methods.

	Guarded hot plate method	Cyclic heat method	Laser flash method	Hot wire method
Classes of methods	Steady-state method	Transient method	Transient method	Transient method
Merit	It can measure the materials with low thermal conductivity.	It can measure the materials at high temperature.	It has short measuring time and small specimen.	It can measure the thermal conductivity directily.
Demerit	It needs long measuring time.	It needs long measuring time.	It preferred densed specimen.	Its results include information of various directions.

(1) Guarded hot plate (GHP) method

The guarded hot plate (GHP) method is a steady-state measuring method to determine the thermal conductivity directly. Fig. 1.5 shows the schematic image of the apparatus. In the principle, it is supposed that the heat flow direction in specimen is one-directional [35]. In regard to the assumption, the apparatus has the guard heater. The heat generated in the metering section heater, cannot transfer to the guarded heater and the specimen's edge [36]. The thermal conductivity λ can be determined from the following equation [35]:

$$\lambda = \frac{Q \cdot \mathrm{d}}{\theta h - \theta c} \tag{1.4}$$

Where Q is the heat flow, d is the specimen thickness, θ_h and θ_c are the temperature of hot and cold surfaces of the specimen, respectively.

(2) Cyclic heat method

Cyclic heat method is one of the transient methods to measure the thermal property. The method is applicable to measure the thermal property in higher temperature ranges and low atmospheric conditions. The previous report [37] explains the apparatus can measure the thermal insulations in the temperature range from 100 °C to around 1000 °C. It also can measure both in the conditions of atmospheric pressure and vacuum [38]. In general, the cyclic heat method has two ways for measuring the thermal property. One way is to measure the phase lag of generated temperature wave propagating through the specimen. Another is to measure the amplitude decay of the generated temperature wave in the specimen [37]. The physical value of specimen determined from these two ways is the thermal diffusivity. The thermal conductivity is obtained by multiplying the density and the specific heat by the thermal diffusivity [34].

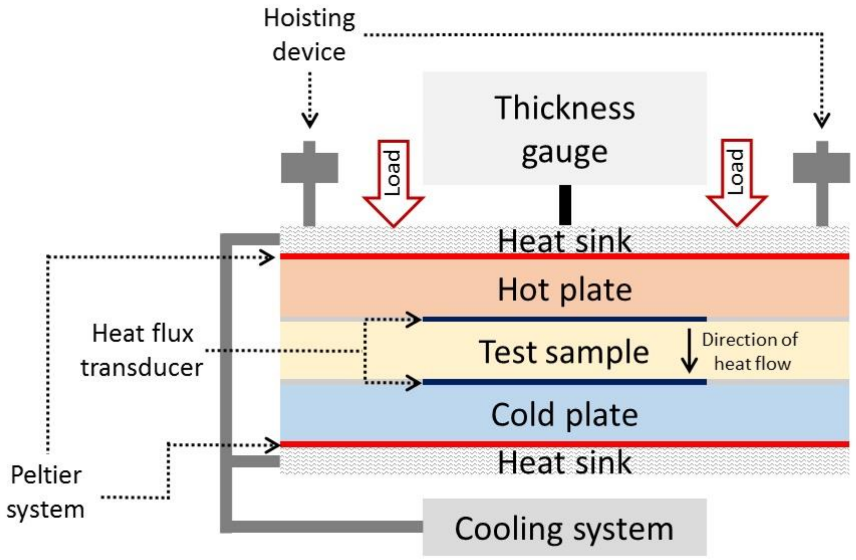

Fig. 1.5 Schematic image of the guarded hot plate (GHP) method apparatus.

(3) Laser flash method

Laser flash method is a widely used method to measure the thermal diffusivity of solid specimen above room temperature [31]. The method can measure the size of mm order solid materials in wide temperature ranges (room temperature to around 1500 °C). The advantage of using this technique includes small specimen size and short measuring time (as a few minutes) [39]. Fig. 1.6 shows the ideal measuring principle of the laser flash method. As a laser beam is spotted onto a solid disc in vacuum condition, a pulse heat is applied to the specimen. At the same time, the temperature change at the back of the specimen is monitored. The temperature rise with time corresponds to the thermal energy diffusion along the thickness direction in the specimen. Therefore, the thermal diffusivity along the thickness for specimen disc can be obtained [31]. The thermal diffusivity α is calculated from the following equation:

$$\alpha(\mathrm{T}) = 0.1388 \times \frac{\mathrm{d}^2}{\mathrm{t}_{1/2}} \tag{1.5}$$

The above equation is obtained from solving a temperature distribution equation [31] of a thermally insulated solid specimen of thickness d at time t. Where T is the measuring temperature, d is the thickness of specimen, $t_{1/2}$ is the time needed for the back of the specimen to reach half of the maximum temperature after pulse heating. One of the features of the laser flash method is that it can measure the wide range of materials such as insulators, semi-conductors, and metals. In addition, the method is based on the thermal diffusive phenomenon in one-dimension.

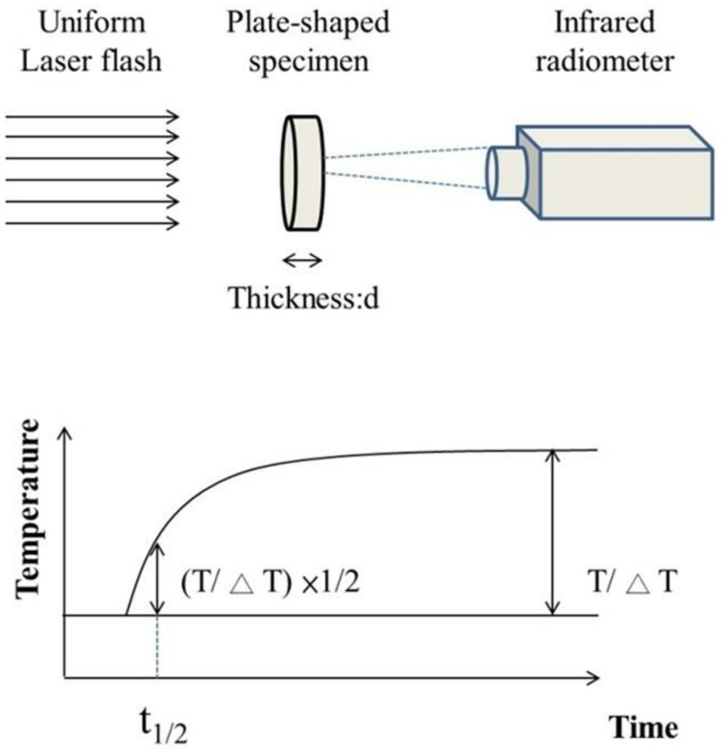

Fig. 1.6 Schematic image of the measuring principle of the laser flash method.

(4) Hot wire method

Unlike to other transient methods, the hot wire method can measure the thermal conductivity directly. Fig. 1.7 shows the schematic image of the hot wire method. The method needs hot wire inside the test specimen as the heat source. It is supposed that a specific quantity of heat Q is generated from the wire, and flows to the radial direction uniformly in the specimen. The thermal conductivity λ is determined from the following equation [40]:

$$\lambda = \frac{Q}{4\pi}\frac{\ln(\frac{t2}{t1})}{\Delta\theta} \tag{1.6}$$

In the equation, t_1 and t_2 are certain different times after the heat is generated from the source. $\Delta\theta$ is temperature difference of a point in the time interval between t_1 and t_2. The point is set at certain distance from heat source.

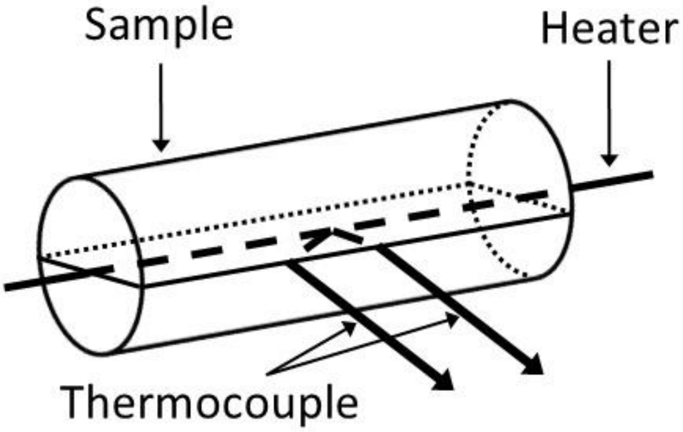

Fig. 1.7 Schematic image of the hot wire method.

1.4.2 Introduction of measuring methods of specific heat capacity

The specific heat capacity (Cp) is one of the physical values in thermodynamics. Not similar to the thermal conductivity and thermal diffusivity, the specific heat capacity depends on the composition of materials and is not sensitive to the structure of the materials. Commonly, it is possible to find precise literature values of the specific heat capacity [41]. For the development of thermal insulation materials, it is one of the important performance indices. However, generally measuring the specific heat capacity of the thermal insulation materials is difficult. This is because they have usually high porosity with very low thermal conductivity and small specific heat capacity [42]. In this study, the following two representative methods are employed to measure the nanoporous thermal insulation materials:

(1) Drop method

In previous report, Ohmura et al developed a newly designed specific heat capacity measuring apparatus by using the drop calorimeter method [43,44]. The apparatus include the heater and water tank. At first, the water tank is kept at room temperature. After the heated specimen (10 mm × 10 mm × 10 mm) was dropped into tank, the water will reach higher equilibrium temperature. The specific heat capacity is then evaluated from measuring the temperature rise of the water tank. The measurement can be applied in the temperature range from 100 °C to around 1000 °C [45].

(2) DSC method

In thermodynamics, differential scanning calorimetry (DSC) is a reliable method to determine the specific heat capacity of materials. In measuring, the sample and reference material are set at sample holders. They are heated or cooled constantly at the same time by the heaters. In DSC method, the individual heaters are needed for both sample and holders [46]. The temperature difference ΔT between the sample and the reference is measured. Then, the heaters are controlled the temperatures of them to achieve the condition of ΔT reaching zero. Thus, both of their temperatures are controlled to the same point. The apparatus records the difference between the quantities of heats supplied to the sample and that supplied to the reference. The result is recorded as a function of temperature or time. One of the features of using DSC method is that the measured specimen is small. Besides, the material such as powder is also available for the measurement by DSC.

1.4.3 Introduction of measuring the strength of nanoporous compact

In this study, the fracture strength measurement of nanoporous compact was conducted by a three-point bending test, using a universal testing machine. The following shows the measuring principle. The dimensions of the test specimens were 100 mm × 30 mm × 10 mm, cut from the compact carefully by cutting tool. The inner span was set at 80 mm; the crosshead speed was set at 1 mm/min. After measuring the fracture load, the flexural strength σ was estimated by using the following equation.

$$\sigma = \frac{3 \times P \times s}{2 \times w \times d^2} \tag{1.7}$$

In the equation, σ is the flexural strength, *P* the fracture load, *s* the inner span, *w* the width of specimen, and *d* the thickness of specimen. In the test, 3 specimens of each condition were measured at room temperature.

In previous study [24], the relation between the three-point bending strength and porosity of the nanoporous fumed silica compact is investigated. The study revealed that the bending strength decreased with increasing the porosity while the porosities ranged from 0.82 ~ 0.90. And the decreasing tendency became significantly with the porosity higher than 0.87. Such tendency can also be found in the condition of powder with aggregated structure. That is to say, the weak secondary aggregated particle structure was destroyed particularly with slightly increasing of the forming pressure. The densification referred to the contacts of primary particles increased significantly in resultant compact. From the result, it indicates that the strength of the nanoporous compact board may be determined by the number of contact points and adhesion forces among the coated silica layer surfaces on fibers [16].

1.5 Objective of this study

1.5.1 Objective

Although, the previous studies proposed the new processing method to prepare advanced nanoporous materials for high performance thermal insulation board [16,17], more details of processing conditions and mechanisms to control the thermal and mechanical properties of the compact still need to be made clear. For instance, to produce the better thermal insulation board by such processing method, controlling the surface morphology of (nanoparticle/fiber) composite particle is important. Therefore, changing the particle properties such as surface properties (hydrophilic surface or hydrophobic surface) or species are of interesting challenges. Besides, the effects of mechanical processing parameters such as processing time and rotating speed on the thermal and mechanical properties of resultant compact board should be more discussed. To achieve these subjects, further research works are conducted in this study. The scope of the thesis is shown as below.

1.5.2 Scope of thesis

The thesis consists of 5 chapters. In Chapter 1, the general introduction of this study and the objectives are explained.

In Chapter 2, it is focused on the surface properties of nanoparticles used to make the porous compact board. As a typical example, the effect of the hydrophilic or hydrophobic surface structure of fumed silica particles on the thermal conductivity and mechanical strength of the resultant compact board is investigated.

In the first part of Chapter 3, a new method to obtain thermal conductivity by using small porous compact board is introduced. A laser flash method is applied to measure the thermal diffusivity of porous thermal insulation material at room temperature. Small sample size and short measuring time are major advantages of this method. In addition, a differential scanning calorimetry (DSC) is applied to measure the specific heat capacity of the sample. With known density, the thermal conductivity at room temperature is finally obtained. The results are compared with the data so far published in the paper. Consequently, it is concluded that this method is promising for rapid measurement of low thermal conductivity materials at room temperature.

In the second part of Chapter 3, the effect of addition ratio of hydrophobic silica to hydrophilic silica on the thermal conductivity of the fibrous silica compacts is investigated. The measurement is conducted using the method introduced in the first part. The effect of the above ratio on the mechanical property of the compacts is also investigated.

In the first part of Chapter 4, a method to measure the thermal conductivity of specimen is introduced. It enables us to measure it from room temperature up to 350 °C by the simple structure. The thermal conductivity of porous compact board is measured by this method. Consequently, it is made clear that this method shows good agreement of the thermal conductivity with that obtained by the cyclic heat method.

In the second part of Chapter 4, aiming at developing a thermal insulation compact board which is available at higher temperature, fumed alumina nanoparticles, ceramic fibers and silicon carbide (SiC) powder are used as starting materials for the porous compact board. Mechanical processing parameters to make the composite fibers by using them are examined. The thermal conductivity is measured by the apparatus introduced at the first part. The effect of the processing conditions on the thermal conductivity and mechanical strength of the resultant compact is evaluated, and the subjects for the developments of thermal insulation porous compact for higher temperature are discussed.

In Chapter 5, the conclusions obtained through this study are summarized.

References

[1] P. M. Cox, R. A. Betts, C. D. Jones, S. A. Spall, I. J. Totterdell, Nature 408 (2000) 184-187.

[2] A. B. Stambouli, E. Traversa, Renewable and Sustainable Energy Reviews 6 (2002) 433-455.

[3] M. Reim, W. Korner, J. Manara, S. Korder, M. Arduini-Schuster, H. P. Ebert, J. Fricke, Solar Energy 79 (2005) 131-139.

[4] G. S. Wei, Y. S. Liu, X. X. Zhang, F. Yu, X. Z. Du, International Journal of Heat and Mass Transfer 54 (2011) 2355-2366.

[5] T. W. Clyne, I. O. Golosnoy, J. C. Tan, A. E. Markaki, Philosophical Transactions of the Royal Society A: Mathematical, Physical and Engineering Sciences 364 (2006) 125-146.

[6] A. R. Studart, U. T. Gonzenbach, E. Tervoort, L. J. Gauckler, Journal of the American Ceramic Society 89 (2006) 1771-1789.

[7] E. Gregorová, W. Pabst, Z. Sofer, O. Jankovský, J. Matějíček, Journal of Physics: Conference Series 395 (2012) 012-022.

[8] R. Liu, Y. Li, C-A Wang, S. Tie, Materials and Design 63 (2014) 1-5.

[9] M. Naito, H. Abe, A. Kondo, T. Yokoyama, C. C. Huang, KONA Powder and Particle Journal 27 (2009) 130-141.

[10] Y. Fukumori, H. Ichikawa, T. Uemura, K. Sato, H. Abe, M. Naito, Proceedings of 8th International Symposium on Agglomeration, Bangkok, Thailand (2005) 31-38.

[11] K. Sato, H. Abe, T. Misono, K. Murata, T. Fukui, M. Naito, Journal of the European Ceramic Society 29 (2009) 1119-1124.

[12] E. Nakamura, A. Kondo, T. Kozawa, H. Abe, M. Naito, J. Yoshida, S. Nakanishi, H. Iba, Journal of the Society of Powder Technology, Japan 51 (2014) 131-135.

[13] T. Kozawa, A. Kondo, E. Nakamura, H. Abe, M. Naito, H. Koga, S. Nakanishi, H. Iba, Materials Letters 132 (2014) 218-220.

[14] E. Nakamura, A. Kondo, M. Matsuoka, T. Kozawa, M. Naito, H. Koga, H. Iba, Journal of the Society of Powder Technology, Japan 52 (2015) 630-634.

[15] D. Tahara, Y. Itoh, T. Ohmura, H. Abe, M. Naito, Ceramic Transactions 146 (2004) 173-177.

[16] H. Abe, I. Abe, K. Sato, M. Naito, Journal of the American Ceramic Society 88 (2005) 1359-1361.

[17] I. Abe, K. Sato, H. Abe, M. Naito, Advanced Powder Technology 19 (2008) 311-320.

[18] Y-G. Kwon, S-Y. Choi, E-S. Kang, S-S. Beak, Journal of Materials Science 35 (2000) 6075-6079.

[19] J. Kuhn, T. Gleissner, M. C. Arduini-Schuster, S. Korder, J. Frike, Journal of Non-Crystalline Solids 186 (1999) 291-295.

[20] D. R. Smith, J. G. Hust, National Institute of Standards and Technology, NISTIR 89-3901, U.S. (1989).

[21] D. R. Smith, in: Thermal Conductivity, C. J. Creers and H. A. Fine (Eds), Plenum Press, New York 21 (1990) 261-276.

[22] M. Naito, A. Kondo, T. Yokoyama, ISIJ International 33 (1993) 915-924.

[23] T. Fukui, K. Murata, S. Ohara, H. Abe, M. Naito, K. Nogi, Journal of Power Sources 125 (2004) 17-24.

[24] T. Ohmura, I. Abe, Y. Ito, K. Sato, H. Abe, M. Naito, Journal of the Society of

Powder Technology, Japan 46 (2009) 461-466.

[25] T. Ohmura, Y. Ito, I. Abe, H. Abe, M. Naito, Journal of the Society of Powder Technology, Japan 46 (2009) 806-812.

[26] H. Barthel, M. Heinemann, M. Stintz, B. Wessely, Chemical Engineering & Technology 21 (1998) 745-752.

[27] T. Ohmura, M. Tsuboi, M. Onodera, T. Tomimura, The reports of Institute of Advanced Material Study Kyushu University 16 (2002) 13-17.

[28] T. Ohmura, J. Nyumura, K. Tsukahara, Processing of the 8th Asian Thermophysical Properties Conference (2007).

[29] A. J. Slifka, Journal of Research of the National Institute of Standards and Technology 105 (2000) 591-605.

[30] D. Kraemer, G. Chen, Review of Scientific Instruments 85 (2014) 025108.

[31] W. J. Parker, R. J. Jenkins, C. P. Butler, G. L. Abbott, Journal of Applied Physics 32 (1961) 1679-1684.

[32] J. J. Healy, J. J. de Groot, J. Kestin, Physica 82C (1976) 392-408.

[33] David G. Cahill, Review of Scientific Instruments 61 (1990) 802-808.

[34] J. M. Ziman, Oxford University Press, Oxford (2001).

[35] ISO 8302, (1991).

[36] T. Ohmura, Proceedings of the 3rd International Forum on Heat Transfer, Nagasaki, Japan (2012).

[37] T. Ohmura, M. Tsuboi, M. Onodera, T. Tomimura, 24th International Congress of the Aeronautical Sciences (2004).

[38] H.S. Carslaw, J. C. Jaeger, Oxford University Press, New York (1959).

[39] M. Akoshima, B. Hay, M. Neda, M. Grelard, International Journal of

Thermophysics 34 (2013) 778-791.

[40] J. Jackson, J. Adams, R. C. Millar, Thermal Transmission Measurements of Insulation: A Symposium, ASTM STP 660, R. P. Tye. Ed. (1997) 154-171.

[41] Y. S. Touloukian, C. Y. Ho, Thermophysical Properties of Matter- the TPRC Data Series, Plenum, New York 5 and 6 (1970/1978).

[42] Thermophysical Properties Handbook, Japan Society of Thermophysical Properties, Yokendo, Tokyo (1990) 544.

[43] Netsu Busseichi Sokuteihou, Japan Society of Mechanicl Engineering (1991) 138-146.

[44] Thermophysical Properties Handbook, Japan Society of Thermophysical Properties, Yokendo, Tokyo (1990) 546.

[45] T. Ohmura, M. Tsuboi, T. Tomimura, Netsu Bussei 17 (2003) 9-17.

[46] K. D. Maglić, A. Cezairliyan, V. E. Peletsky, Compendium of Thermophysical Property Measurement Methods 1 (1984) 669-685.

Chapter 2

Effect of Fumed Silica Surface Properties on the Thermal Insulation Performance of Fibrous Silica Compacts

Abstract

The particle's surface properties play an important role in developing advanced thermal insulation compact made by fumed silica. In this chapter, the effect of using hydrophilic or hydrophobic particles on the thermal conductivity and strength of the resultant insulation compact board was investigated. A higher thermal conductivity and higher strength were obtained in using hydrophilic silica particles. Very low thermal conductivity, below 0.02 W/m·K, was reached in using hydrophobic silica particles. The difference of thermal conductivity was mainly affected by solid part. The decrease of thermal conductivity and the increase of strength were related to the bonding condition between particles in the compact.

2.1 Introduction

The issues of energy-saving and reduction of CO_2 emissions are very important recently. High performance thermal insulation is one of the key to solve these problems. For example, the silica aerogel prepared by supercritical drying is a promising material. It shows nanoscale porous structure which leads to the extremely low thermal conductivity. But, there are several problems of using this material for thermal insulation. The thermal insulation compact board made of silica aerogel is very fragile. Besides, the thermal insulation ability of silica aerogel decreases at high temperature range [1].

In recent research, the fumed silica has been used for thermal insulation field. The thermal conductivity of the compacts made of fumed silica is near that of silica aerogels. It is mainly attributed to high porosity and the nanoscale porous structure in the compact. To improve the mechanical property, the glass fibers were added to increase the strength of resulted compacts. A dry mechanical processing method was also developed to fabricate fiber reinforced fumed silica compact. The silica nanoparticles were first coated onto the fiber to form fumed silica/glass fiber composite. Then, the processed powder mixtures were compacted to form the thermal insulation board [2,3]. By using such mechanical treatments, the nanoscale pores remained in the compact. This method minimizes the fiber-fiber contacts through the coating of silica. Therefore, a highly uniform dispersion of fibers in the compact was achieved. For controlling the thermal conductivity at high temperature, the SiC particles were added to decrease the radiation heat transfer of the compact.

Although the compacts show excellent thermal insulation ability, the effect of the particle properties on the performance is still unclear. In this chapter, the fumed silica nanoparticles with hydrophilic or hydrophobic characteristics were employed. The effect of surface characteristics on the thermal conductivity and strength of the resulted compact board are discussed.

2.2 Experimental procedure

2.2.1 Sample preparation

The starting materials were hydrophilic type fumed silica powder (AEROSIL300, Nippon Aerosil, Tokyo, Japan), hydrophobic type fumed silica powder (AEROSILR812, Nippon Aerosil, Tokyo, Japan), glass fibers (CS3J-888, Nittobo, Tokyo, Japan) and SiC powder (Silcar-Gl, Wacker Chemie, Münich, Germany). The specific surface area S_{BET} of the hydrophilic and hydrophobic fumed silica, determined by BET method (3Flex Surface Characterization Analyzer, Micromeritics Japan, Chiba, Japan), was 300 m^2/g and 250 m^2/g, respectively. Through the use of surface area, the equivalent size, d_{SW}, of hydrophilic and hydrophobic silica was respectively 10 nm and 12 nm. The fumed silica powder showed a three-dimensional nanoscale chain-like aggregated structure with spaces of several tens nanometers [2,3], as shown in Fig. 2.1 (a) [2]. The glass fibers were added to reinforce the strength of the compact. The alkali content of the aluminum borosilicate glass fiber is less than 1 mass%. The diameter and length of the fibers were 10 μm and 3 mm, respectively, as shown in Fig. 2.1 (b). The SiC powder was added to reduce the radiation heat transfer of the compact. The average diameter of SiC, as determined from a particle size analyzer (Microtrac MT3300 EXII, NIKKISO, Tokyo, Japan), was 3.3 μm, and its morphology was shown in Fig. 2.1 (c).

Table 2.1 shows the chemical composition of the powder mixtures. The mass ratio of fumed silica (hydrophilic or hydrophobic): glass fibers: SiC in the 100 g powder mixtures was 60:20:20. The mixture was then mechanically processed by the horizontal axis type shearing mixer (Hosokawa Micron Corp., Osaka, Japan), as shown in Fig. 1.2, without media ball in dry phase. The processing time and rotating speed were 10 min and 1000 rpm, respectively. There was a certain clearance between the rotating rotor and chamber [4]. When the blade rotating, powder mixture was compressed into the clearance through compressive and shear forces, despite no media ball was present. In experiment, the clearance between the rotor and chamber was 3 mm. After the processing, the fumed silica/glass fiber powder mixture was obtained. The powder mixture was then uniaxially pressed to form the compact (100 mm × 150 mm × 10 mm) by using the pressure of 2 MPa. The approximate temperature and humidity of atmosphere during the mechanical processing and pressing were 25 °C and 50 %, respectively. The compact made of hydrophobic silica was heat treated at 400 °C for 12 hs to evaluate the effect of hydrophobic surface group on the properties of the board.

Table 2.1 Chemical composition of the silica thermal insulation board.

Material	Compounding ratio (mass%)	Average diameter
Fumed silica nanoparticle (Hydrophilic or hydrophobic)	60	10 nm (Hydrophilic) 12 nm (Hydrophobic)
Glass fiber	20	10 μm
SiC particle	20	3.3 μm

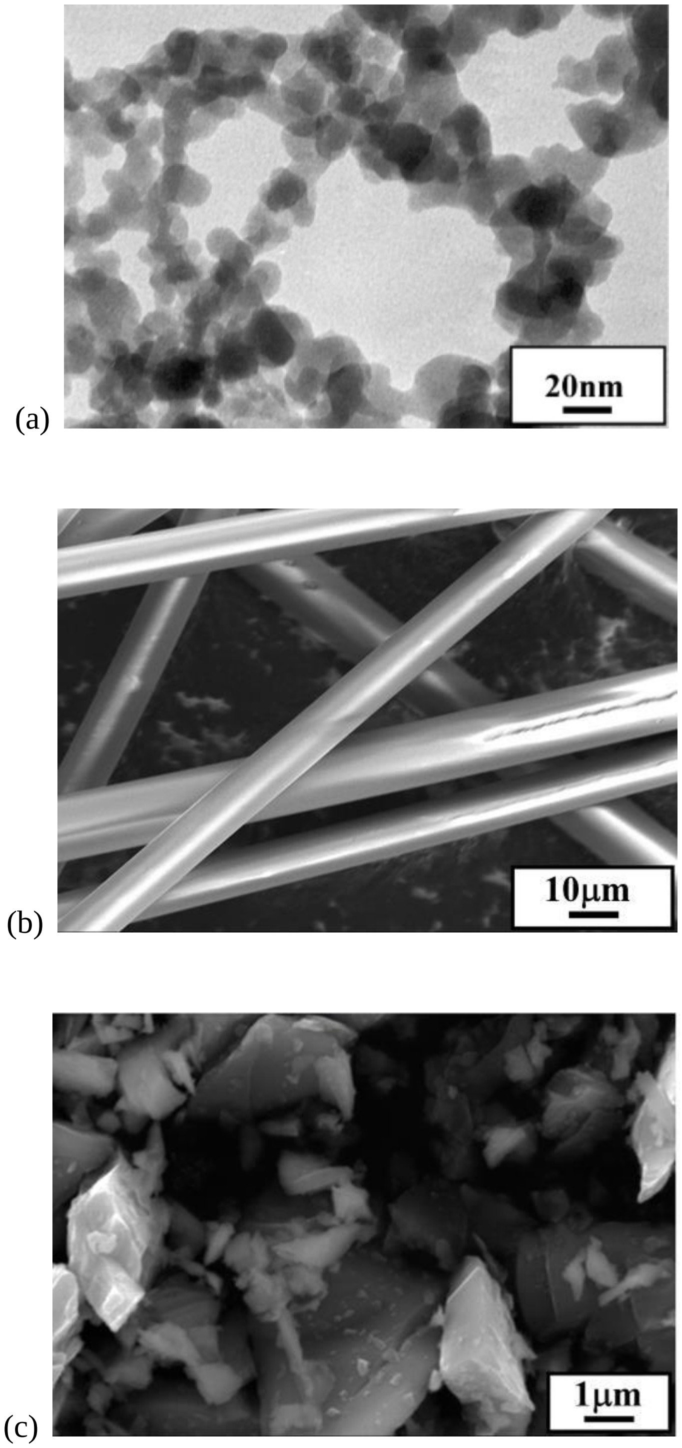

Fig. 2.1 Starting materials: (a) TEM image of fumed silica powder [2], (b) SEM image of glass fibers and (C) SiC particles.

2.2.2 Sample characterizations

The microstructure of processed fibers was observed by using scanning electron microscopy (SEM, JSM-6010LA, JEOL Ltd., Tokyo, Japan). To evaluate the surface characteristics of processed powders, the IR transmittance of the powder mixtures before and after processing was determined by FTIR spectrometer. The apparent density and porosity of the compact was determined by measuring its dimensions and weight. Three samples were measured for each composition.

The thermal diffusivity was measured by a cyclic heat method [5]; and the specific heat capacity by a drop calorimeter method [5]. The thermal conductivity was determined from thermal diffusivity, specific heat capacity and density at the temperature range from 100 °C to 600 °C. The measurement was carried out three times for each board. In this chapter, the thermal conductivity under atmosphere was measured first, and then measured under vacuum condition (around 1 Pa). The thermal conductivity of a compact consists of nanostructure under atmosphere was evaluated by using the following equation [6,7]:

$$\lambda = A\rho + B\,\mathrm{T}^3/\rho + \lambda_g \tag{2.1}$$

where ρ is the density (kg/m^3), T the absolute temperature (K), λ_g the thermal conductivity of gas (W/(m·K)), A the coefficient of solid part of thermal conductivity and B the coefficient of radiation part, respectively. The thermal conductivity under vacuum condition was proposed as following:

$$\lambda_v = A\rho + B\,\mathrm{T}^3/\rho \tag{2.2}$$

On the plot of the third power of absolute temperature and thermal conductivity under vacuum, the intercept was given as $A\rho$ and the slope as B/ρ. The values of A and B were then obtained experimentally. From the difference between thermal conductivity under atmosphere and vacuum conditions, the thermal conductivity contributed by the gas part inside of the nanopores was determined.

Three-point fracture strength measurement using a universal testing machine was applied. The dimensions of the specimens were 10 mm in thickness, 30 mm in width and 100 mm in length. A load cell of 500N type was used in the measurement. A crosshead speed of 1 mm/min with an inner span length of 80 mm was used. Three specimens for each board were measured.

2.3 Results

2.3.1 Microstructure observation and density measurement

Figure 2.2 (a) and (b) shows the morphology of coated silica-layers on the glass fiber composite using hydrophilic and hydrophobic silica particles after the mechanical processing, respectively. The layer formed by nanoparticles coated well on the glass fiber, as shown in the figures. When using hydrophilic silica, the coated layer was thicker than that of using hydrophobic one. During the mechanical processing, the hydrophilic particles adhere onto the glass fiber and form a first layer, and then other particles adhere onto the first layer to increase its thickness. For hydrophobic particles, only a thin layer was coated on the fibers after the processing. Fig. 2.2 (c) and (d) shows the cross-section of coated fiber with using hydrophilic and hydrophobic silica particles, respectively.

By taking the statistics from SEM images as shown in Fig. 2.1 (b) and Fig. 2.2, the average diameter of raw fiber, fiber with hydrophilic silica layer and fiber with hydrophobic silica layer were 11.0 μm, 15.8 μm and 12.4 μm, respectively. 50 fibers of each composition were calculated. Therefore, the average thickness of coated hydrophilic silica layer and coated hydrophobic silica layer on fibers were around 2.4 μm and 0.7 μm, respectively.

The apparent density and porosity of the prepared fibrous fumed silica compacts are as shown in Table 2.2. All the specimens exhibit around 400 kg/m^3 of their apparent density. The corresponding porosities of them are higher than 85%. Therefore, the compacts with high porosity and light weight structure were obtained by the technique. The slightly decreasing tendency of apparent density of the hydrophobic type compact after heating at 400 °C is may be due to the hydrophobic surface group in material was decomposed during the heat process.

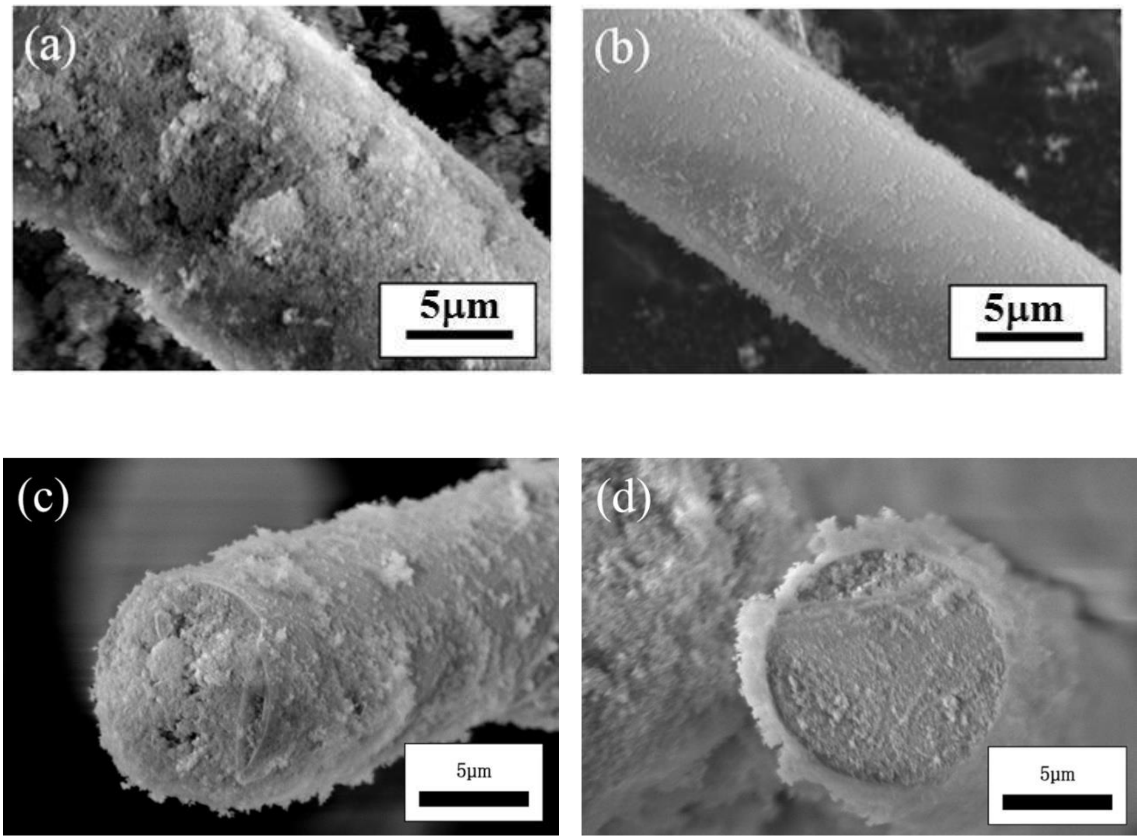

Fig. 2.2 SEM images of the coated glass fibers, (a), (c): glass fiber with hydrophilic silica particles; (b), (d): glass fiber with hydrophobic silica particles.

Table 2.2 Density and porosity of the fibrous fumed silica compacts.

	Apparent density /(STD) (kg/m^3)	Porosity /(STD) (%)
Compact using hydrophilic silica	405 /(4.0)	85.5 /(0.15)
Compact using hydrophobic silica	395 /(3.6)	85.9 /(0.12)
Compact using hydrophobic silica (after heating at 400°C)	384 /(6.5)	86.3 /(0.21)

*STD: Standard deviation.

2.3.2 Thermal conductivity measurement

Figure 2.3 and 2.4 show the results of thermal conductivity of the fumed silica compacts with temperature under atmosphere and under vacuum condition, respectively. In Fig. 2.3, all the values of thermal conductivity are below 0.031 W/m·K. The values change little in the temperature range from 100 °C to 600 °C under atmosphere condition. These results are close to the values of reported silica aerogel [1]. In particular, the thermal conductivity of the compact made by using hydrophobic fumed silica shows an extremely low value, 0.018 W/m·K, below 300 °C. But, while the hydrophobic type compact was heated to 400 °C, the value increases slightly. Nevertheless, its value is still lower than that of the hydrophilic type compact. Fig. 2.4 shows the thermal conductivity measured under vacuum condition. The values are lower than those measured under atmosphere condition.

The thermal conductivities of silica, glass fiber and SiC at room temperature are around 1.4 W/m·K, 2.0 W/m·K and 270 W/m·K, respectively. If the compact was full density, by assuming Rule-of-mixture, the theoretical thermal conductivity is 55 W/m·K. Therefore, the thermal conductivity of the prepared compact was controlled effectively by such tailored nanoporous structure.

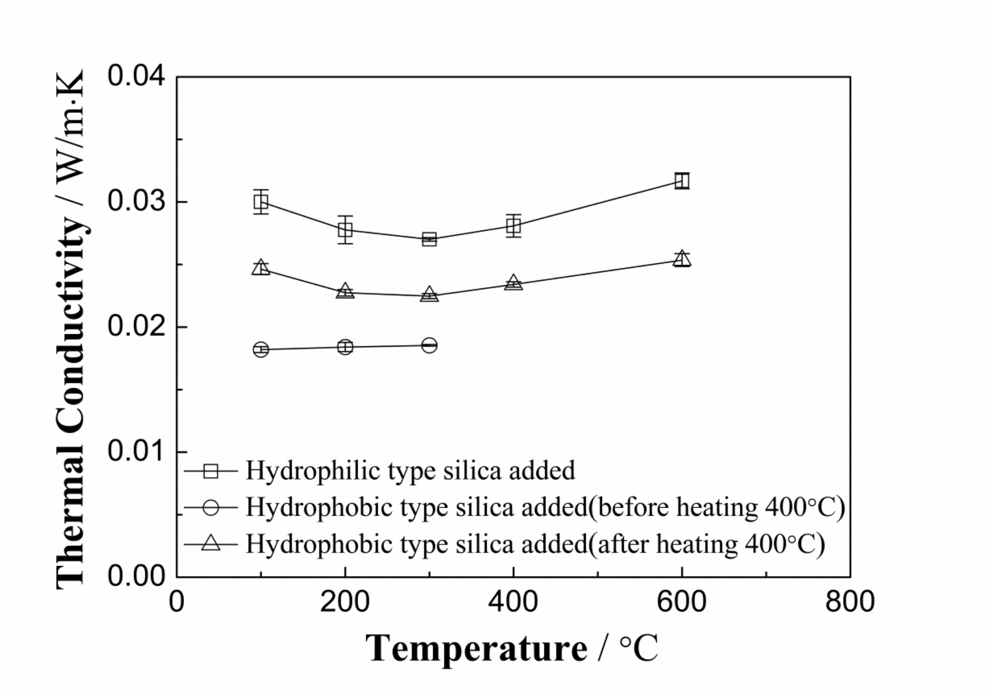

Fig. 2.3 Thermal conductivity of the fibrous fumed silica compacts under atmosphere condition.

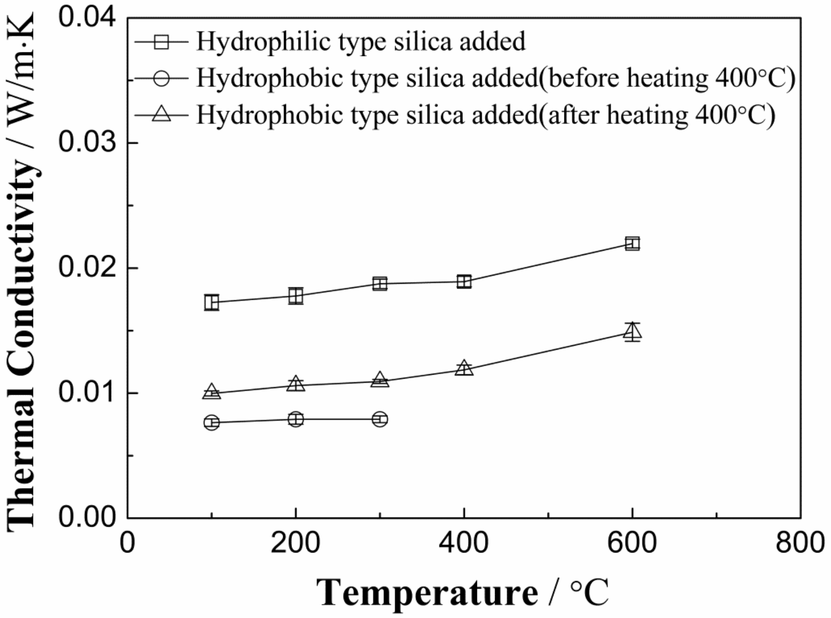

Fig. 2.4 Thermal conductivity of the fibrous fumed silica compacts under vacuum condition.

2.3.3 Strength measurement

In Table 2.3, the compact using hydrophilic silica shows the fracture strength of 0.30 MPa. This strength value is sufficient for the subsequent machining of the compacts compared to conventional fumed silica board [8]. However, the strength of the compact using hydrophobic type silica is only 0.03 MPa. The value is much lower than that of the hydrophilic one. After heating at 400 °C for 12 hs, its strength increases to 0.08 MPa. From the result, it is suggested that the functional group on the surface of silica particle is the key affecting the strength of the resulted compact.

Table 2.3 Fracture strength of the fibrous fumed silica compacts.

	Fracture strength /(STD) (MPa)
Compact using hydrophilic silica	0.30 /(0.007)
Compact using hydrophobic silica	0.03 /(0.001)
Compact using hydrophobic silica (after heating at 400°C)	0.08 /(0.001)

*STD: Standard deviation.

2.3.4 FTIR analysis

Figure 2.5 exhibits the result of IR transmittance for the hydrophilic type silica before and after mechanical processing. More Si-O bondings are found after the mechanical processing. Previous study demonstrated that the converting O atoms and silicon wafer to Si-O bonding needed a temperature above 700 °C in an oxidizing atmosphere condition [9]. However, mechanical processing in this experiment was conducted at room temperature. The mechanical forces during the processing may produce localized high temperature between particles. Other study indicated localized high pressure may assist the phase transformation of lead oxide common rutile form (I) to denser orthorhombic form (II) through the use of mechanical mixer [10]. Therefore, localized high temperature and high pressure could affect the particles to form the chemical bonding of Si-O. Such bonding situation was not observed in the mixture using hydrophobic type silica.

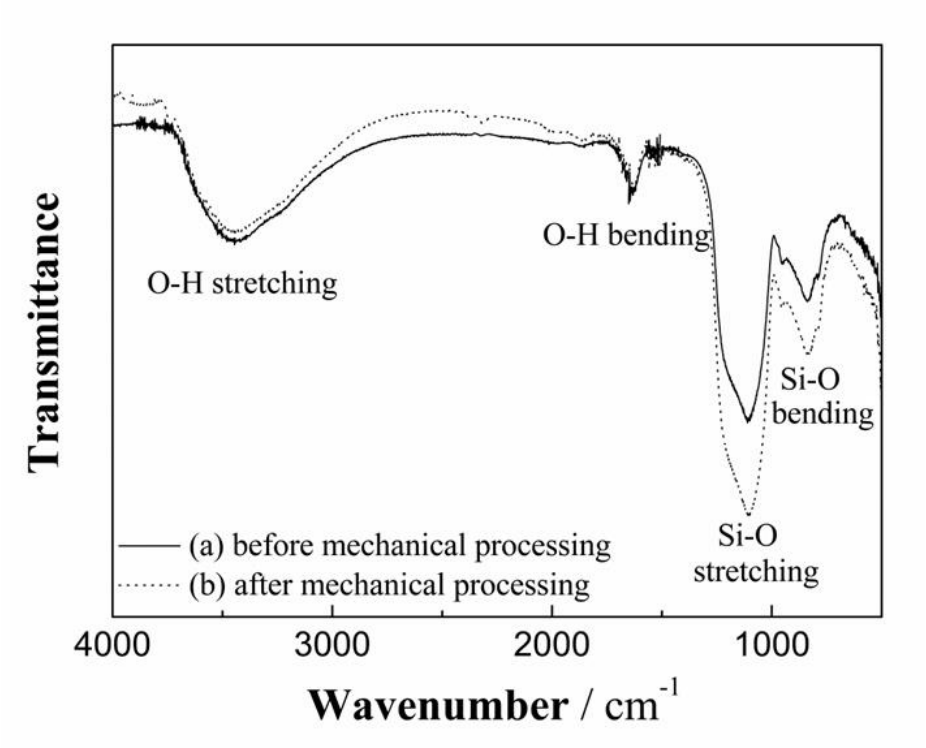

Fig. 2.5 IR transmittance caused by Si-O stretching (a) before and (b) after the mechanical processing for the mixture using hydrophilic type silica.

2.4 Discussion

2.4.1 Analysis of thermal property

In order to analyze the thermal conductivities of the compact using hydrophilic and hydrophobic silica, the knowledge on three parts, the heat transfer in solid, the effect of radiation, and the heat transfer in gas is needed. Fig. 2.6 shows the relation between the third power of absolute temperature and thermal conductivity of the compacts under vacuum condition. In this figure, the linear relationships are observed. According to Eq. (2.2), the intercept shows $A\rho$ and the slope shows B/ρ. With known density, the values of A and B are obtained. Table 2.4 shows the coefficients A, $A\rho$ and B of the resulted compacts.

From Table 2.4, the coefficient "A" of the compact using hydrophilic silica was much higher than that of hydrophobic one. The value of $A\rho$ for the hydrophilic type is twice as much as that for the hydrophobic one. This indicates that the difference in thermal conductivity of solid part is affecting the thermal conductivities of both compacts. On the other hand, the coefficient "B" is related to the radiation part. The relationship between BT^3/ρ and measuring temperature is plotted in Fig. 2.7. The value of BT^3/ρ shows very low below 300 °C. Therefore, the thermal conductivity of the compact affected by radiation below 300 °C is very small. While the temperature is higher than 400 °C, BT^3/ρ increases slightly with increasing measuring temperature. It can be related to the addition of SiC powders. The thermal conductivity of the insulation boards increases slightly within 300 °C to 600 °C, in Fig. 2.3 and Fig. 2.4.

Figure 2.8 shows the contribution from the gas, λ_g, on the thermal conductivity. The difference between the values for three kinds of boards is small. Thus, the difference of thermal conductivity was not affected by the part contributed from gas. As a result, it is suggested that the difference of thermal conductivity is mainly resulted from the solid part of thermal conductivity in the compact.

Such hypothesis can be supported with the result of IR measurement. As in Fig. 2.5, Si-O bonding is formed in hydrophilic type silica after mechanical processing. It means the silica particles easily form chemical bonding to other silica or glass fiber in this situation. It results in thicker silica layer after mechanical processing. The thick silica layer on the surface of processed fibers produces the strong bonding with other fibers and particles. It leads to higher thermal conductivity for hydrophilic type silica compact. Such type of bonding mechanism was not found in the hydrophobic one.

Table 2.4 Coefficients of *A* and *B* for the compacts.

	A /(STD) $(\mathrm{W \cdot m^2/(kg \cdot K)})$	*A*ρ /(STD) $(\mathrm{W/(m \cdot K)})$	*B* /(STD) $(\mathrm{W \cdot kg/(m^4 \cdot K^4)})$
Compact using hydrophilic silica	4.3×10^{-5} /(1.2×10^{-6})	0.0170 /(0.00049)	2.8×10^{-9} /(6.1×10^{-10})
Compact using hydrophobic silica	2.0×10^{-5} /(2.6×10^{-7})	0.0076 /(0.00010)	0.8×10^{-9} /(5.8×10^{-10})
Compact using hydrophobic silica (after heating at 400°C)	2.5×10^{-5} /(5.1×10^{-7})	0.0096 /(0.00020)	3.1×10^{-9} /(3.9×10^{-10})

*STD: Standard deviation.

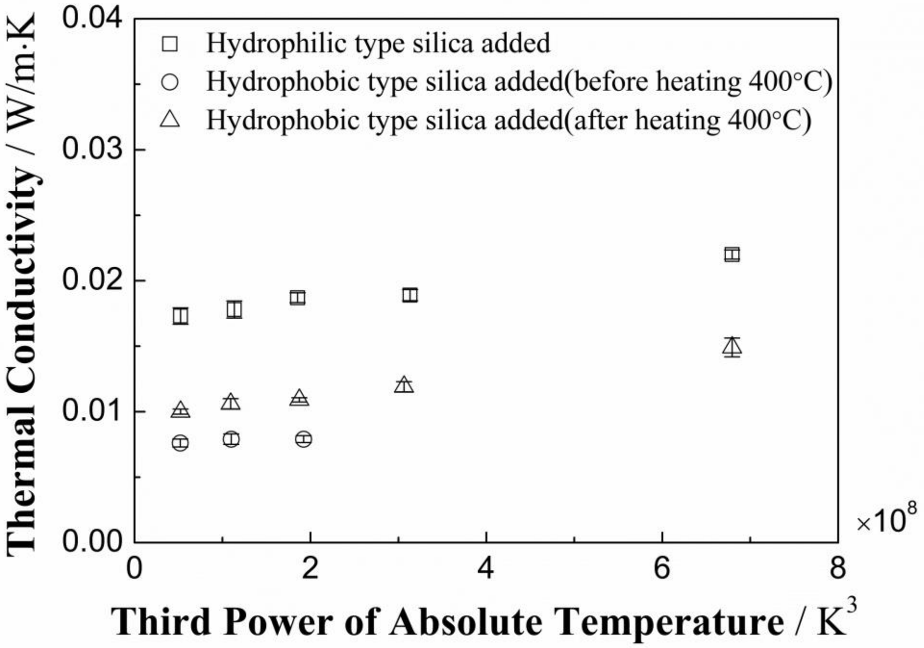

Fig. 2.6 Relation between the third power of absolute temperature and thermal conductivity of the compacts, under vacuum condition.

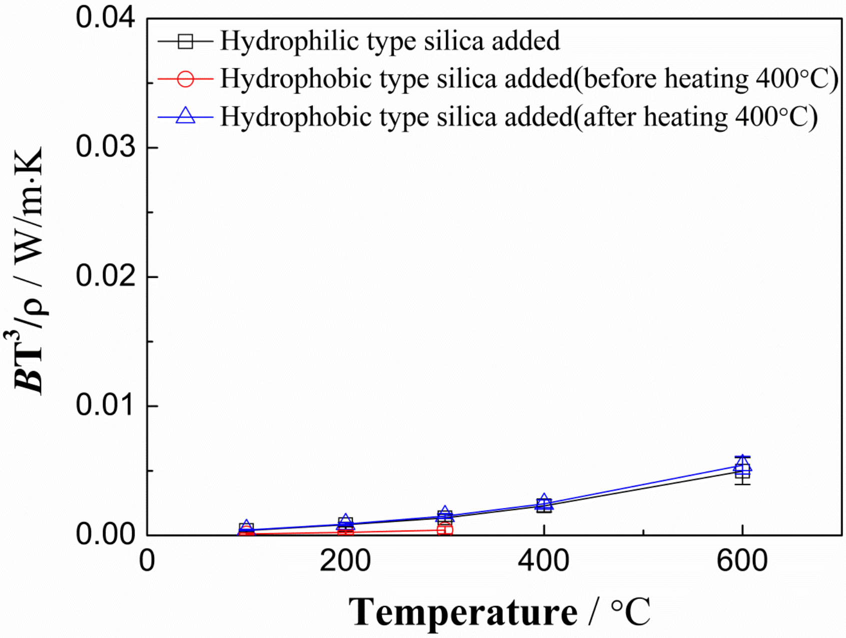

Fig. 2.7 Relation between $B\,T^3/\rho$ and measuring temperature.

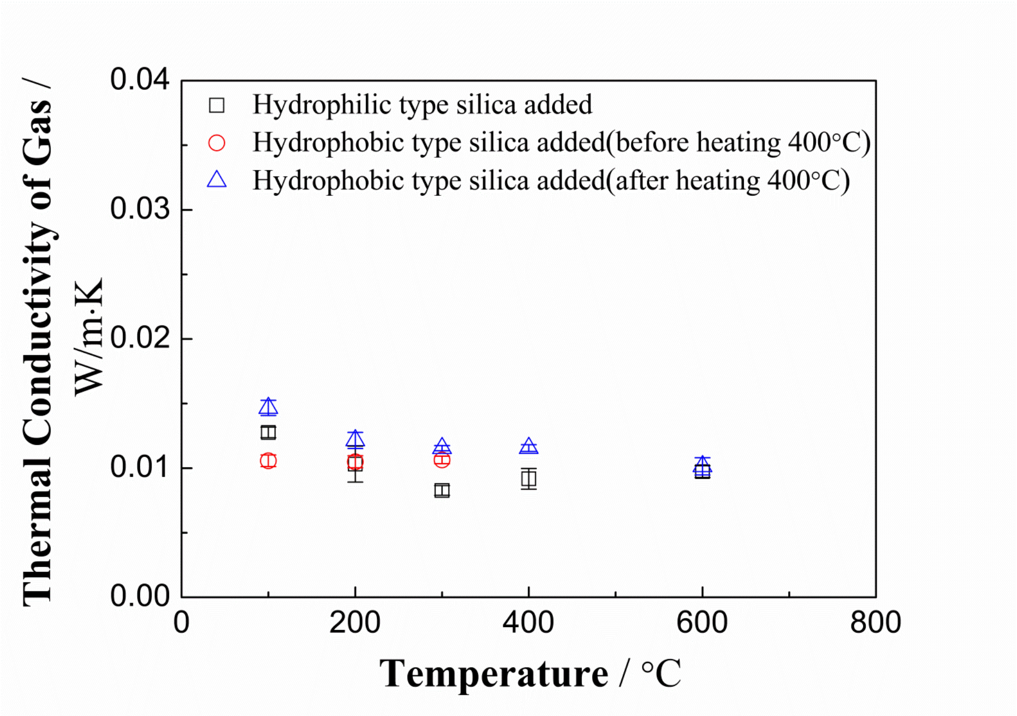

Fig. 2.8 Relation between thermal conductivity of gas and measuring temperature.

2.4.2 Analysis of mechanical property

The strength of the compact using hydrophilic silica was much higher than that of using hydrophobic one. The surface of glass fiber is hydrophilic. The higher strength can be related to the strong bonding between glass fiber-fumed silica particles, in adding to that between fumed silica-fumed silica particles. For the board composing of hydrophilic silica, strong Si-O bonding produces higher contact force between fiber-silica and that between silica-silica particles. But, in the hydrophobic type, no chemical Si-O bonding is formed after the mechanical processing. The presence of hydrophobic functional group on silica leads to less chance for the formation of bonding between fiber-silica and that between silica-silica particles. The strength is thus much lower than that of hydrophilic type one.

2.4.3 Effect of heat treatment on the properties of hydrophobic type compact

Both the thermal conductivity and strength of the compact using hydrophobic silica are increased after the heat treatment at 400 °C. Fig. 2.9 shows the IR transmittance for the powder mixture using hydrophobic silica before and after heated 400 °C for 12 hs. The C-H bonding is decreased after heating, as in the figure. It indicates the hydrophobic methyl group is decomposed. The hydrophobic functional group may reduce the contact force between particles. After its decomposition, the contact force would increase. Thus, although the density of the hydrophobic type compact is decreased slightly after heating, the compact shows a higher strength. A larger contact area would also lead to the result of higher thermal conductivity.

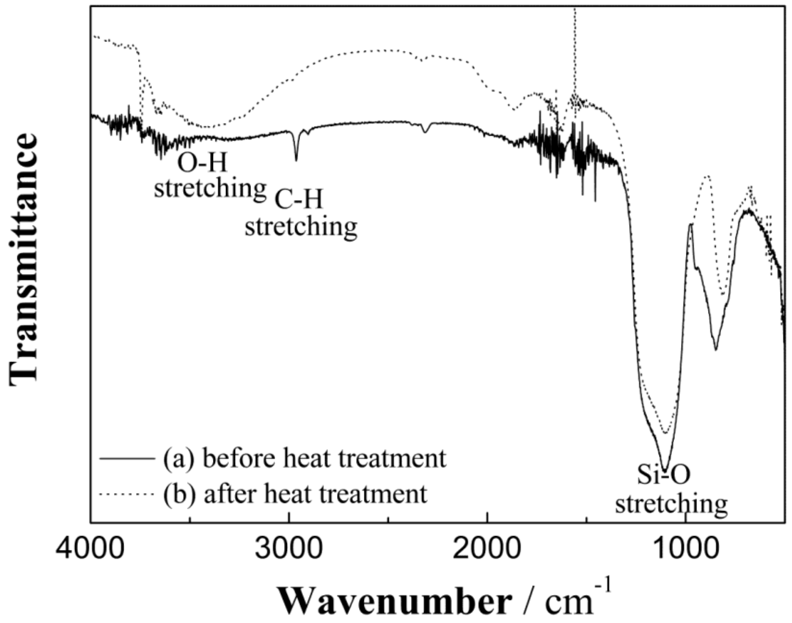

Fig. 2.9 IR transmittance of the processed powder mixture using hydrophobic type silica powder (a) before and (b) after 400 °C heat treatment for 12 hs.

2.5 Conclusions

(1) The fiber reinforced fumed silica board with low thermal conductivity, light weight, and machining-ability was successfully prepared.

(2) The thermal conductivity and strength of the compact boards were affected by the characteristics of used silica particles.

(3) Higher thermal conductivity and higher strength were obtained for the compact using hydrophilic type silica.

(4) Lower thermal conductivity and lower strength were obtained for the compact using hydrophobic type.

(5) The difference of thermal conductivity of both boards is mainly resulted from the heat transfer between the solid parts.

(6) The Si-O bonding between particles in the boards plays an important role. The difference of strength is resulted from the bonding between fiber-silica and between silica-silica particles.

References

[1] Y Y-G. Kwon, S-Y. Choi, E-S. Kang, S-S. Beak, Journal of Materials Science 35 (2000) 6075-6079.

[2] H. Abe, I. Abe, K. Sato, M. Naito, Journal of the American Ceramic Society 88 (2005) 1359-1361.

[3] I. Abe, K. Sato, H. Abe, M. Naito, Advanced Powder Technology 19 (2008) 311-320.

[4] M. Naito, A. Kondo, T. Yokoyama, ISIJ International 33 (1993) 915-924.

[5] T. Ohmura, M. Tsuboi, Netsu Bussei 13 (1999) 264-270.

[6] T. Ohmura, M. Tsuboi, M. Onodera, T. Tomimura, The reports of Institute of Advanced Material Study Kyushu University 16 (2002) 13-17.

[7] T. Ohmura, I. Abe, Y. Ito, K. Sato, H. Abe, M. Naito, Journal of the Society of Powder Technology, Japan 46 (2009) 461-466.

[8] D. R. Smith, in: Thermal Conductivity, C. J. Creers and H. A. Fine (Eds), Plenum Press, New York 21 (1990) 261-276.

[9] J. B. Lasky, Applied Physics Letters 48 (1986) 78-80.

[10] F. Dachille, R. Roy, Nature 186 (1960) 34.

Chapter 3

Effect of Addition Ratio of Hydrophobic Silica to Hydrophilic Silica on the Thermal and Mechanical Properties of Fibrous Silica Compacts

Abstract

In the first part of this chapter, a rapid measuring method to obtain thermal conductivity by using porous compact is proposed. A laser flash apparatus and a differential scanning calorimetry (DSC) are applied to determine the thermal properties. The result of obtained thermal conductivity is compared with the other data. In the second part of this chapter, the effect of addition ratio of hydrophobic silica to hydrophilic silica on the thermal conductivity of the fibrous silica compacts is investigated. The measurement was conducted using the method explained in first part. The thermal conductivity of fibrous silica compacts is 0.042 W/m·K. The addition of 5% hydrophobic silica further reduces the value to 0.033 W/m·K. The thermal conductivity decreases slightly with increasing hydrophobic silica content. The strength also decreases with the increase of hydrophobic silica. A compromise between the thermal insulation ability and mechanical strength is needed. The performance of fibrous silica compacts shows strong dependence on the surface structure of glass fibers.

3.1 The development of rapid thermal conductivity measuring method of porous thermal insulation material by laser flash method

3.1.1 Introduction and background of laser flash method

High performance thermal insulation materials are usually porous and have very low thermal conductivity. The determination of the thermal conductivity for such material is the important issue for their development. However, to measure the materials with low thermal conductivity is challenging.

Generally, there are two ways to measure the thermal conductivity: steady-state method and transient method [1-5]. Steady-state method gives a thermal gradient to the test specimen, and measures the thermal conductivity directly. The method is frequently used to measure the thermal conductivity of thermal insulation material. However, the method needs relatively large specimen and long measuring time [1,2]. On the other hand, transient method provides transitional thermal flow to test specimen, and then determines the thermal conductive properties from the response of the temperature change [3-5]. The heating modes, such as pulse heating method, cyclic heating method, and laser flash heating method are frequently used. In particular, the laser flash heating mode is widely used. The technique uses small specimen; and the measuring time can be as short as a few minutes [3]. But, the transient methods only determine the thermal diffusivity; therefore, the specific heat capacity and density data are needed for calculating the thermal conductivity.

Figure 1.6 shows the principle and the theoretical temperature rise curve as a result from the laser flash method. As a laser beam is spotted onto a solid disc in vacuum condition, a pulse heat is applied. The change of temperature at the back of the specimen is monitored simultaneously. The temperature rise with time corresponds to the thermal energy diffusion along the thickness direction, in the specimen. Thus, the thermal diffusivity along the thickness direction can be obtained [3]. The thermal diffusivity α is determined from the following equation:

$$\alpha(\mathrm{T}) = 0.1388 \times \frac{\mathrm{d}^2}{\mathrm{t}_{1/2}} \tag{3.1}$$

Where T is the measuring temperature; d is the thickness of specimen; $t_{1/2}$ is the time needed for the back of the specimen to reach half the maximum temperature after pulse heating, as shown in Fig. 1.6. In order to obtain the thermal conductivity, specific heat capacity of specimen was measured using a differential scanning calorimeter (DSC). It is a reliable method to determine the specific heat capacity. The method also has the features of using small specimen [6].

So far in this research field, G. Wei et al measured the thermal insulation material of xonotlite-type calcium silicate by a conventional laser flash apparatus. The thermal conductivity of xonotlite around 0.064 W/m·K was determined in their report [7]. However, in present method, the advanced porous insulation material with much lower thermal conductivity was successfully measured by using laser flash method and DSC method. The data is compared with that obtained in Chapter 2.

3.1.2 The details of rapid thermal conductivity measuring process

(1) Preparation of the test specimen

The detail for the preparation of the test specimen with nanoporous structure is similar to the specimen prepared in Chapter 2 [8]. A brief preparation procedure is given here. The starting materials were fumed silica powder (AEROSIL300, Nippon Aerosil, Tokyo, Japan), glass fiber (CS3J-888, Nittobo, Tokyo, Japan) and SiC powder

(Silcar-G1, Wacker Chemie, Münich, Germany). The specific surface area of the fumed silica was 300 m^2/g. Its particle size was 10 nm. The silica powder showed a nano chain-like structure with the size of several tens nanometers [9,10]. The length and diameter of the fiber were 3 mm and 10 μm, respectively. The average particle size of SiC was 3.3 μm.

The ratio (mass%) of fumed silica: glass fibers: SiC in the powder mixture was 60:20:20. A mechanical processing was applied for the starting powder mixture. The processing time was 10 min. The mixing device composed of main chamber, and certain clearance between the rotating rotor and chamber [11], as shown in Fig. 1.2. The applied rotating speed was 1000 rpm. The processed powder was uniaxially pressed to form the bulk compact (100 mm × 150 mm × 10 mm) with pressure of 2 MPa. The temperature and humidity of atmosphere during the processing were around 25 °C and 50%, respectively. By measuring the compact’s dimensions and weight, its apparent density and porosity were determined.

(2) The laser flash measuring process

The test specimen for the thermal diffusivity and heat capacity measurement was cut from prepared porous compact. The thermal diffusivity was measured by laser flash apparatus (LFA-502N, Kyoto Electronics Manufacturing CO., LTD, Japan) at room temperature (near 300 K), in air. The size of the specimens was 10 mm in diameter and 2.5 mm in thickness. Due to the nanoporous compact is very fragile, the cutting process should be cautious. First the thin board with 2.5 mm thickness was cut from the compact carefully, by using sawing machine. Then the belt punch with 10 mm diameter was used to cut the specimen from the thin board. The thickness of specimen was measured by a linear gauge (Litematic, VL-50A, Mitutoyo CO., Japan). It was measured five times at different locations. Before measurement, the specimen surface was coated by carbon spraying. The thermal diffusivities of 4 samples (specimen #1- #4) were measured. In experiment, the power for laser pulse heating was controlled. For the specimens #1 and #2, the laser beam was changed in three different power levels. Specimens were measured five times at each level and the apparent thermal diffusivity was obtained. For the specimens #3 and #4, the laser beam was changed in four different power levels. Specimens were measured two times at each level.

(3) The DSC measuring process

Specific heat capacity was measured by a differential scanning calorimeter (DSC, PerkinElmer Co., USA). The specimen mass, diameter, and thickness were 15 mg, 5 mm, and 1.4 mm, respectively. The DSC pans and covers were made of aluminum. The specimens were heated up to 200 °C on the hot plate for 4h-5h before measuring. The standard material was sapphire (α-Al_2O_3). Atmosphere was the flowing dry nitrogen (20 ml/min). Specific heat capacity of 1 specimen was measured 5 times, and the measuring temperature was ranged from -10 °C to 390 °C. In 5 times measurements, the heating rates were set at 10 K/min for 2 times and 20 K/min for 3 times.

3.1.3 Reliability of the developed rapid thermal conductivity measuring method

The density and porosity of the test specimen for the thermal diffusivity and specific heat measurement were 413 kg/m^3 and 85.3 %, respectively. Fig. 3.1 shows a temperature rise curve for the specimen #1 by laser flash. The vertical axis was normalized by the maximum temperature rise. From the figure, the curve was smooth, indicating that the test specimen had uniform composition. Comparing the curve with the theoretical temperature rise curve as shown in Fig. 1.6, the large heat loss effect was found. In general, during laser heating, the thermal energy may be lost through heat transfer by radiation (radiation), sample holder (conductive heat transfer), and to the air (convective heat transfer) etc. Therefore, it is necessary to correct the heat loss effect before determining the thermal diffusivity. The curves were corrected using a methodology proposed by Cape and Lehman [12]. The corrected curve is also shown in Fig. 3.1. After the correction, the apparent thermal diffusivity is obtained from Eq. (3.1). However, the obtained apparent thermal diffusivity value still included factors such as the temperature dependence and the apparatus constant. For eliminating these factors, the following method was used.

During the measuring, the power for laser pulse heating was changed in several different power levels. Different laser power results in different temperature rise pattern. The relation between apparent thermal diffusivity and temperature rise (ΔT) was shown in Fig. 3.2. At first, the right side curve in Fig. 3.1 was curve-fitted, and obtained the intercept of the fitted curve at time = 0. The intercept was then defined as temperature rise (ΔT). Its value depends on the power of laser beam. As proposed by M. Akoshima et al [13], the thermal diffusivity is obtained from the intercept at zero of temperature rise, in Fig. 3.2. The different gradients of lines are also observed in the figure. In the report of M. Akoshima et al, the gradients are affected by the specimen thickness and the surface condition such as coating [13]. Due to above factors, the gradients of lines changed although the specimens were made by the same thickness material. The result of thermal diffusivity at room temperature (300K) is shown in Table 3.1. The major uncertainties for the value for thermal diffusivity include the uncertainty of specimen thickness, half time, and measuring temperature. The average thickness of each specimen was also shown in the Table 3.1. The standard deviation of the thickness was around 3 %. According to Eq. (3.1), the uncertainty in specimen thickness contributes around 6% to the uncertainty in the thermal diffusivity. Considering the above uncertainties, the effective figures of the measured thermal diffusivity are 2 digits. From Table 3.1, the obtained thermal diffusivities are around 1.2×10^{-7} m^2/s ~ 1.4×10^{-7} m^2/s. Thus the average thermal diffusivity of the specimens (specimen #1- #4) is 1.3×10^{-7} m^2/s. The standard deviation of the thermal diffusivity was 1.2×10^{-8} m^2/s. From the result of measurement, it is suggested that the reproducibility of this method is high.

The average specific heat capacity measured by DSC method at 300 K is 0.721 J/K·g. From above results, the thermal conductivity of the specimen was obtained by multiplying the density, thermal diffusivity and specific heat capacity [3]. Therefore, thermal conductivity of the nanoporous material is 0.039 W/m·K, at 300 K. It is almost the same as that for silica aerogels [14]. In Chapter 2, the thermal conductivity obtained by cyclic heating method was 0.030 W/m·K at 100 °C. Comparing the results, it suggests that the laser flash method can produce a reliable measurement.

Table 3.1 Thermal diffusivity measured by laser flash method at 300 K.

	Average thickness (mm)	Standard deviation of thickness (mm)	Thermal diffusivity (m^2/s)
Specimen #1	2.304	0.050	1.2×10^{-7}
Specimen #2	2.522	0.065	1.4×10^{-7}
Specimen #3	2.331	0.066	1.2×10^{-7}
Specimen #4	2.564	0.039	1.4×10^{-7}

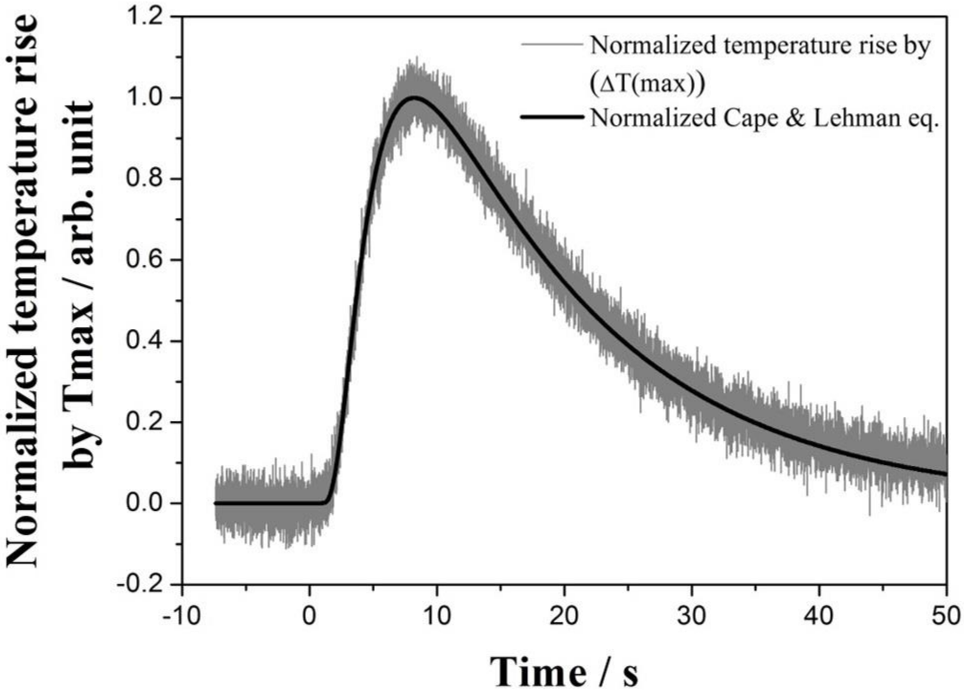

Fig. 3.1 Temperature rise curve for the specimen #1.

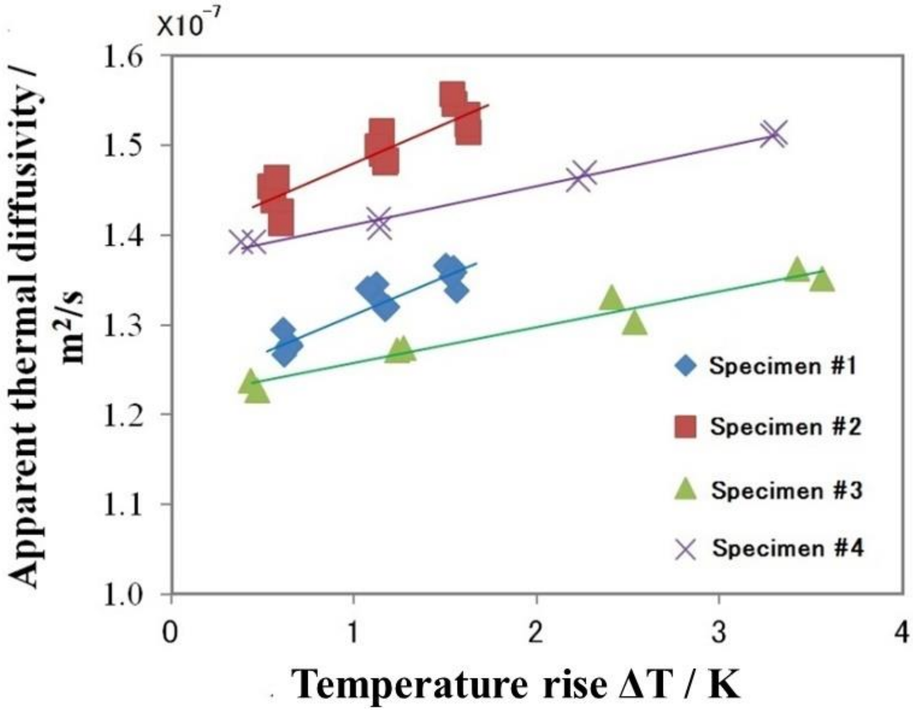

Fig. 3.2 Apparent thermal diffusivity as a function of temperature rise (ΔT).

3.1.4 Superiority of the rapid thermal conductivity measuring method

In this section, rapid measurement of the thermal diffusivity of porous thermal insulation material by laser flash method was demonstrated. The specific heat capacity was determined by DSC method. Thermal conductivity was obtained from the results of density, thermal diffusivity, and specific heat capacity. Thermal conductivity of the nanoporous test specimen is 0.039 W/m·K, at room temperature. The thermal conductivities obtained by the laser flash method and DSC method exhibits good agreement with the data obtained by conventional methods (conducted in Chapter 2). It suggests the proposed method is very promising for rapid measurement of very low thermal conductivity materials.

3.2 The effect of addition amount of hydrophobic silica nanoparticles on the thermal insulation of fibrous silica compacts

3.2.1 Introduction

In recent years, global warming and heat pollutions are becoming serious problems to the world. To insulate the heat sources more effectively is one of the solutions to these problems. As explained in Chapter 2, advanced fibrous silica compacts for thermal insulation is successfully fabricated using a mechanical process. From the results, the obtained thermal conductivity shows dependence on the type of silica. As the compacts made of hydrophilic silica powder and of hydrophobic silica powder were measured by cyclic heat method [8], the compact composing of hydrophobic silica showed higher thermal insulation ability than that of hydrophilic one, in the measuring temperature range from 100 °C to 300 °C. However, the strength of the compact with hydrophobic silica showed a low strength value of 0.03 MPa, which was only 1/10 of the compact with hydrophilic silica. Therefore, the mixing of both types of silica particles to prepare the thermal insulation compact is an interesting subject for the improvement of strength. Present section focuses on the effect of hydrophobic silica nanoparticles addition on the thermal property of the fibrous silica compacts. The measurement was conducted by a laser flash/DSC method developed in first part of this chapter. The mechanical property of the compacts was also investigated.

3.2.2 Experimental procedure

(1) Sample preparation

The starting materials were hydrophilic fumed silica powder (AEROSIL300, Nippon Aerosil, Tokyo, Japan), hydrophobic fumed silica powder (AEROSILR812, Nippon Aerosil, Tokyo, Japan), and glass fibers (CS3J-888, Nittobo, Tokyo, Japan). The specific surface area of hydrophilic and hydrophobic silica powder was respectively 300 m^2/g and 250 m^2/g, as determined by the BET method (3Flex Surface Characterization Analyzer, Micromeritics Japan, Chiba, Japan). The equivalent size of hydrophilic and hydrophobic silica particles was 10 nm and 12 nm, respectively. The diameter and length of the glass fibers were around 10 μm and 3 mm, respectively.

Table 3.2 shows the chemical composition of the fibrous silica compacts. The mass ratio of fumed silica powder (hydrophilic and hydrophobic particle) and glass fibers in 100 g mixture was 75 to 25. For the part of fumed silica, the hydrophobic silica content was selected 0%, 5%, 10%, 30% and 50%, respectively. The starting powders were treated by a mechanical process using the horizontal axis type shearing mixer (Hosokawa Micron Corp., Osaka, Japan) [11], as shown in Fig. 1.2. The mixing time and rotating speed were set at 10 min and 1000 rpm, respectively. The environmental temperature and humidity were set at around 25 °C and 50%, respectively. After the processing, the silica/fiber composite powder was obtained. The microstructures of the processed powder mixtures were observed by scanning electron microscopy (SEM, JSM-6010LA, JEOL Ltd., Tokyo, Japan). The processed powder was then pressed to form the thermal insulation compact board [15] (100 mm × 150 mm × 10 mm) by using a uniaxial pressure of 2 MPa. The density and porosity of the compact were calculated using the dimensions and weight. One compact for each composition was measured. In addition, the inner structure of the compact was observed by SEM.

Table 3.2 Chemical composition of the fibrous silica compacts.

Material	Compounding ratio (mass%)	Average diameter
Hydrophilic and hydrophobic silica	75	10 nm (Hydrophilic) 12 nm (Hydrophobic)
Glass fiber	25	10 μm (length: 3 mm)

(2) Sample characterizations

The thermal diffusivity was measured by a laser flash apparatus mentioned in section 3.1 [16]. The specimens with the size of 10 mm in diameter and 2.5 mm in thickness were cut from the compact. Before the measurement, the specimen was dried at 120 °C for 1 day, and each surface was coated by carbon spray. Two or three specimens for each composition were measured. The specific heat capacity was measured by a DSC [6], also mentioned in section 3.1 [16]. The diameter and thickness of the specimen for DSC were 5 mm and 1.5 mm, respectively. The specimen was heated up to 200 °C before measuring. The hydrophobic silica content 0%, 30%, and 50% specimens were measured for 5 to 6 times at the temperature ranged from -10 °C to 390 °C. The thermal conductivity was obtained by multiplying density, thermal diffusivity and specific heat capacity [3].

The strength was determined by a three-point bending test. The dimensions of the specimens were 100 mm × 30 mm × 10 mm, cut from the compact board. The inner span was 80 mm; the crosshead speed was 1 mm/min. Three specimens for each composition were tested.

3.2.3 Results

(1) Microstructure observation and density measurement

Figure 3.3 (a) - (d) shows the morphology of the glass fiber after the 10 min mechanical processing of silica powder and fibers. The hydrophobic silica content varies from 0% to 50%. The fiber was covered with silica nanoparticles after the processing. The fiber with 0% hydrophobic silica shows the thickest coating layer, as shown in Fig. 3.3 (a). In contrast, the fiber with 50% hydrophobic silica exhibits the thinnest coating layer. The thickness of the layer roughly decreases with increasing hydrophobic silica particles content. Such different coating layer structure may be related to different results of thermal conductivity and strength.

Table 3.3 shows the apparent density and porosity of fibrous silica compacts. The compacts exhibit an apparent density around 350 kg/m^3. The density of the compact with 0% hydrophobic content shows a slightly higher value of 375 kg/m^3. The theoretical densities of the silica and glass are near to each other, around 2700 kg/m^3. Thus the porosity in each compact is close to 87%. It indicates that the fibrous silica compacts with high porosity and light weight are successfully prepared.

Figure 3.4 shows the fracture surface of the compacts containing 0% and 50% hydrophobic silica. The fracture surface is perpendicular to the die-pressing direction. The Fig. 3.4 (a) shows a preferred orientation for the glass fibers. The exposed fibers tend to lie on the plane perpendicular to the die-pressing direction. While the hydrophobic content increases to 50%, the micrograph Fig. 3.4 (b) shows a similar structure. It is suggested that the fibers within the compact board form a preferred orientation. Thus, it is expected that the fibers would be pulled out at fractured surface in the bending test.

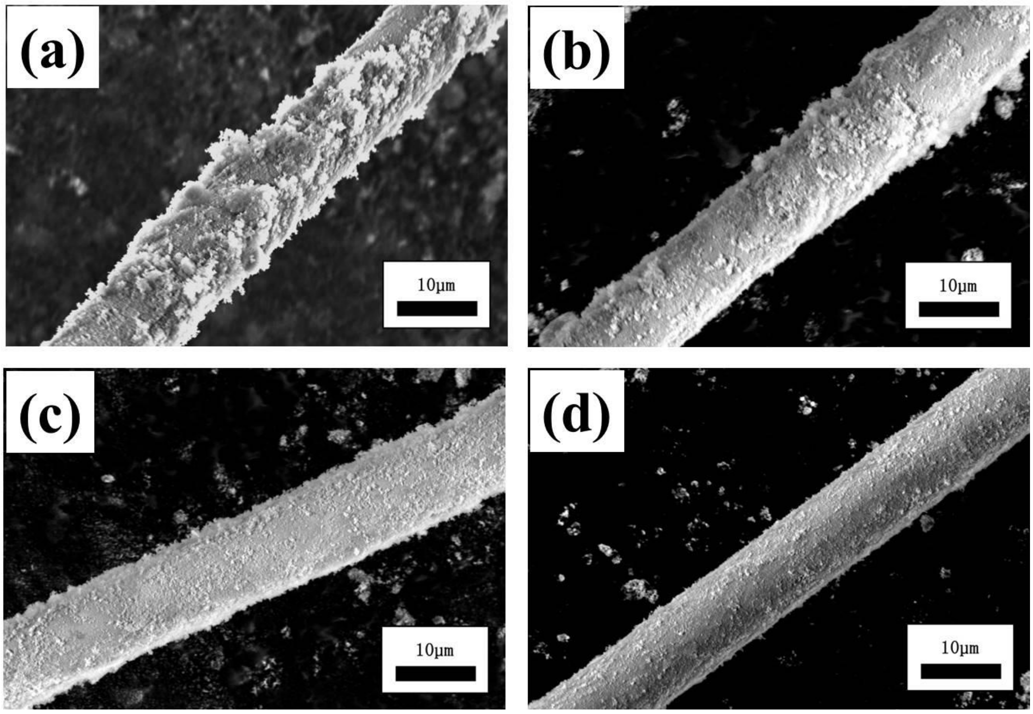

Fig. 3.3 The coated glass fibers with (a) 0%, (b) 10%, (c) 30% and (d) 50% hydrophobic silica after mechanical processing.

Table 3.3 Density and porosity of fibrous silica compacts with various hydrophobic silica contents.

Hydrophobic silica content / %	Apparent density / kg/m^3	Porosity / %
0	375	86.1
5	345	87.2
10	364	86.5
30	344	87.3
50	353	86.9

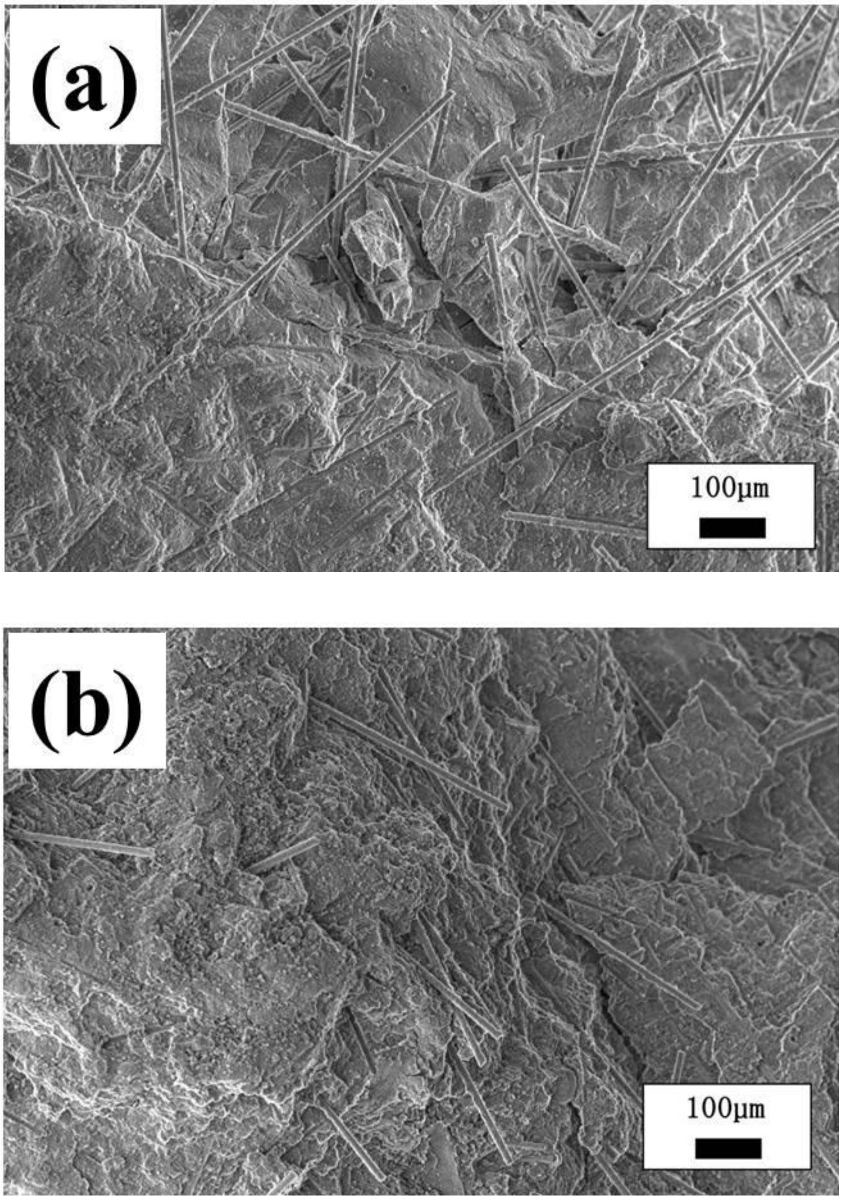

Fig. 3.4 Fracture surface of fibrous silica compacts containing (a) 0% and (b) 50% hydrophobic silica particles.

(2) Thermal property and strength measurement

The specific heat capacity of the specimen with hydrophobic silica content of 0%, 30% and 50% is 0.740 J/K·g, 0.739 J/K·g and 0.746 J/K·g at 300 K, respectively. The average value of 0.742 J/K·g is employed in determining thermal conductivities. Fig. 3.5 shows the obtained thermal conductivity for the compacts with various hydrophobic silica contents. While the hydrophobic silica content was 0%, it has thermal conductivity of 0.042 W/m·K. With the addition of only 5% of hydrophobic silica particles, the thermal conductivity reduces to 0.033 W/m·K. Then, the value decreases slightly with increasing hydrophobic silica content up to 50%. Therefore, it indicates the addition of hydrophobic silica can decrease the thermal conductivity of fibrous silica compacts effectively. If the compact was full density, the theoretical thermal conductivity is 1.6 W/m·K. Thus, similar to result in Chapter 2, the thermal conductivity of prepared compact was controlled effectively by the designed nanoporous structure.

Figure 3.6 shows the result of the strength measurement. Error bars indicates the standard deviations. The strength of the compacts with 0% hydrophobic silica content is 0.44 MPa. The value is high enough to allow subsequent machining. However, with the addition of 5% to 10% of hydrophobic silica, the strength decreased significantly to about 0.18 MPa. Then, it decreased slightly with increasing the hydrophobic silica content up to 50%, and showed a very low value of 0.1 MPa. Comparing the strength result with that obtained in Chapter 2, the strength of compact with 0% hydrophobic silica content (100% hydrophilic silica content) showed higher value in this section. This may be due to the compacts in Chapter 2 containing relatively large SiC particle in structure, and hence its strength decreased. On the whole, the thermal conductivity and strength depends strongly on the amount of added hydrophobic silica in this section.

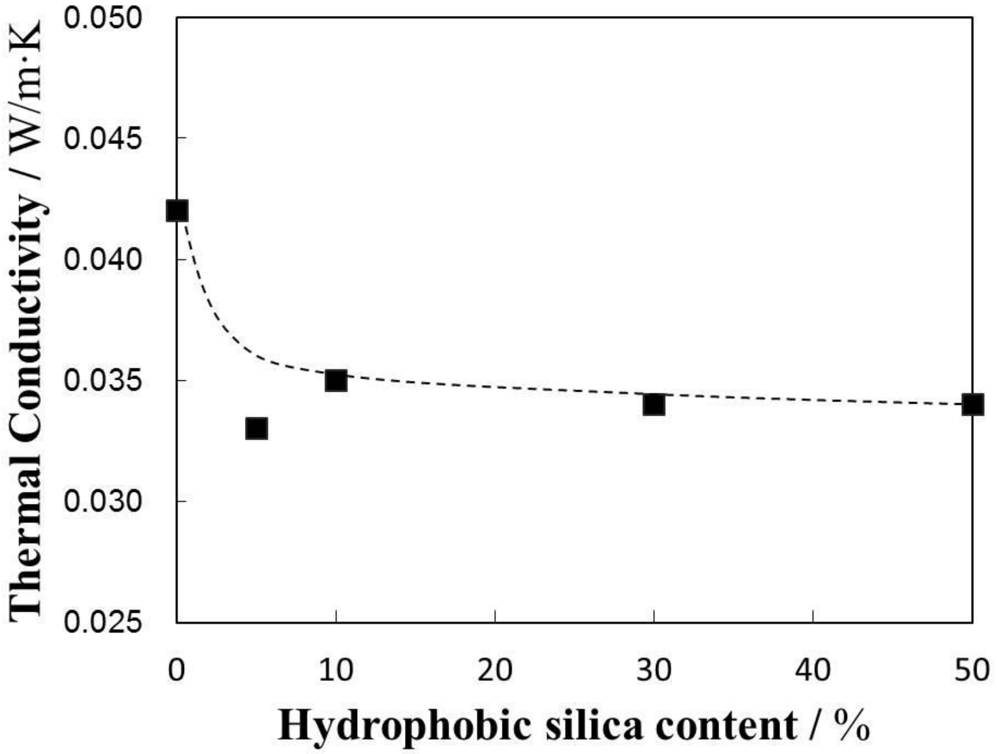

Fig. 3.5 Thermal conductivity of the compacts with various hydrophobic silica contents at 300K.

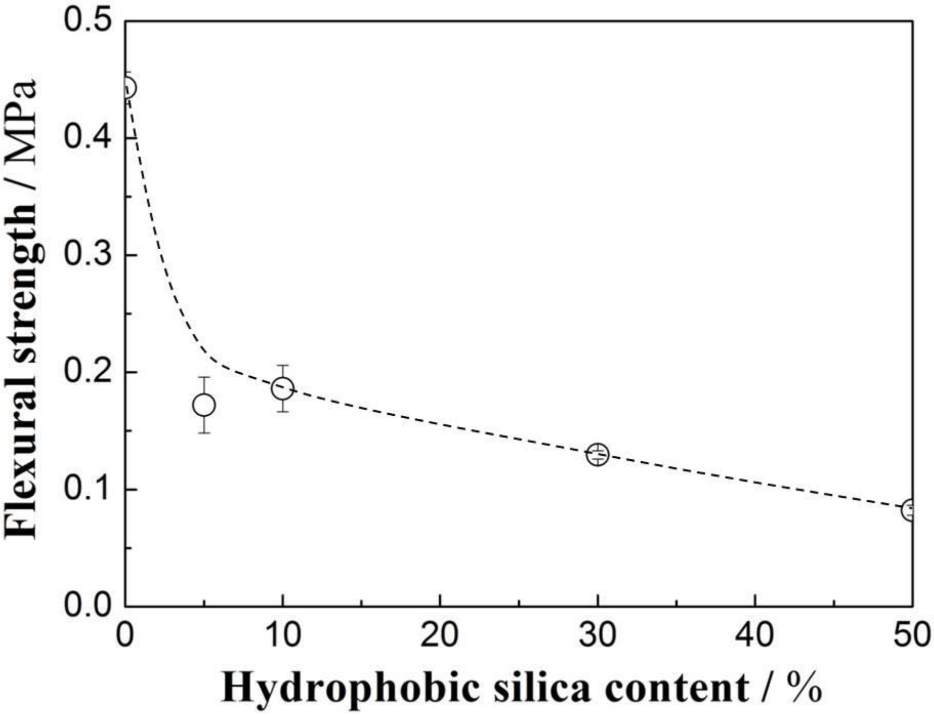

Fig. 3.6 Strength of the fibrous silica compacts with various hydrophobic silica contents.

3.2.4 Discussion

(1) Bonding situations after the mechanical processing

From previous report [17], there are two functional groups, silanol and siloxane, on the surface of hydrophilic silica used in this study. The silanol group with connectivity Si-O-H is a hydrophilic functional group; and the siloxane group with connectivity Si-O-Si is a hydrophobic functional group. The used hydrophobic silica particle is a product prepared from the hydrophilic silica [17]. After treating by hexamethyldisilazane, the surface property of particle changes from hydrophilic to hydrophobic type. A previous research [18] indicated that the density of silanol on the surface of hydrophilic silica in this study is 2.2 SiOH/nm^2. After the treatment, the density decreased to 0.54 SiOH/nm^2; thus the surface property shifted to hydrophobic type.

Figure 3.7 shows the schematics for the interactions between the silica particles after the mechanical processing. While the hydrophobic content is 0%, as shown in Fig. 3.7 (a), the Si-O-Si bonding between silanol groups can be formed easily after obtaining mechanical energy from the processing, which is high enough to cause dehydration condensation reaction between OH groups [8,10]. It increases the contacts between silica particles. In contrast, as shown in Fig. 3.7 (b), with the addition of hydrophobic particles, the Si-O-Si bonding by hydrophilic Si-OH groups will be sterically hindered by hydrophobic Si-O-Si-$(CH_3)_3$ groups. The contacts between particles may decrease after the processing. It is expected that the contacts between particles will decrease with increasing the hydrophobic silica. Above-mentioned bonding situation is related to the different silica layer structure on processed fibers. As a result, the addition of hydrophobic silica led to a decreased layer's thickness, as shown in Fig. 3.3 (a) - (d).

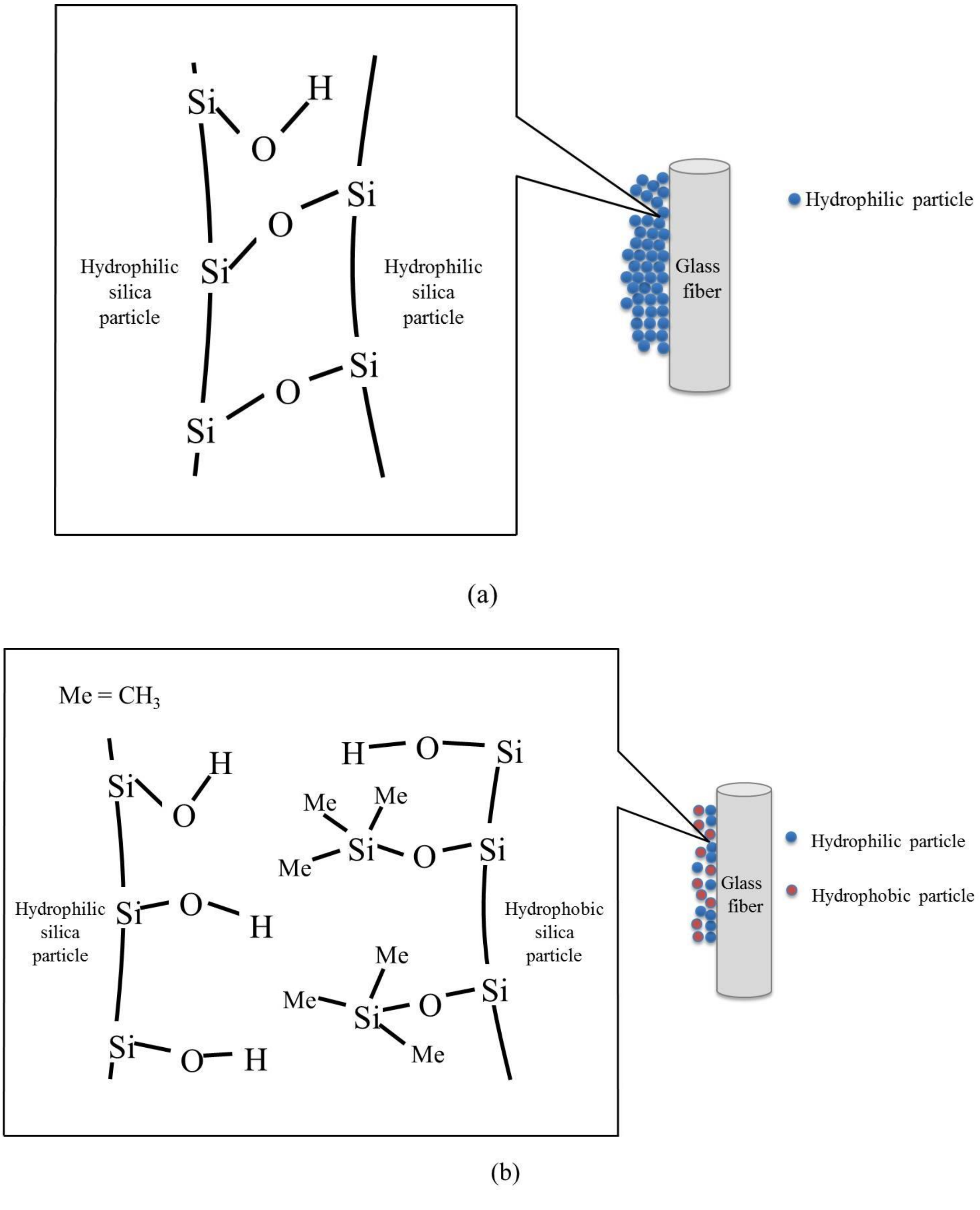

Fig. 3.7 Schematics for fibrous silica composite particles (a) with only hydrophilic particles, and (b) with the mixtures of hydrophilic and hydrophobic silica particles.

(2) Analysis of thermal and mechanical properties

As in Fig. 3.3 (a) - (b), the coated layer amount on the glass fiber surface is decreased with only the addition of 10% hydrophobic silica. It leads to the decreasing of conductive heat transfer of solid part, owing to the decreasing of the contacts between silica particles. While the hydrophobic particle content increases from 10% to 50%, the thermal conductivity keeps low. As shown in Fig. 3.3 (b) - (d), the silica surface layer is similar with each other; therefore, their thermal conductivities are close.

In the strength part, the strength of the compact with 0% hydrophobic silica is decreased by half with 5% - 10% of hydrophobic silica was added. The strength of the compact is mainly dominated by the contacts between fibers and silica particles. From the above-mentioned reason, the contacts between coated fibers decrease due to the addition of hydrophobic particles. Besides, the cohesive force between hydrophilic particles would decrease after the addition of hydrophobic particles. This is because the hydrophobic silica particle has rich Si-CH_3 group on the surface, and the chemical bonding of Si-O-Si is decreased after the hydrophobic silica particles addition. Due to these effects, the mechanical strength of the compact would decrease after the hydrophobic silica addition.

3.3 Conclusions

(1) A rapid measurement of the thermal diffusivity of porous thermal insulation material by laser flash method was demonstrated.

(2) The effect of ratio of hydrophilic to hydrophobic silica on the properties of the fibrous silica compact was investigated. With the addition of only 5% of hydrophobic silica particles, the thermal conductivity decreased from 0.042 W/m·K to 0.033 W/m·K; and decreased slightly with increasing the hydrophobic content up to 50%.

(3) The strength decreased with the addition of 5% hydrophobic silica; then decreased slightly with increasing the content from 10% to 50%.

(4) The change of thermal conductivity and strength was related to the coated surface structure of glass fiber in the resulted compact.

(5) With increasing hydrophobic silica content, the contacts between fiber and particles and the cohesive force between silica particles are decreased. Such decrease tendency results in lower thermal conductivity and lower strength.

References

[1] A. J. Slifka, Journal of Research of the National Institute of Standards and Technology 105 (2000) 591-605.

[2] D. Kraemer, G. Chen, Review of Scientific Instruments 85 (2014) 025108.

[3] W. J. Parker, R. J. Jenkins, C. P. Butler, G. L. Abbott, Journal of Applied Physics 32 (1961) 1679-1684.

[4] J. J. Healy, J. J. de Groot, J. Kestin, Physica 82C (1976) 392-408.

[5] David G. Cahill, Review of Scientific Instruments 61 (1990) 802-808.

[6] K. D. Maglić, A. Cezairliyan, V. E. Peletsky, Compendium of Thermophysical Property Measurement Methods 1 (1984) 669-685.

[7] G. Wei, X. Zhang, F. Yu, K. Chen, International Journal of Thermophysics 27 (2006) 235-243.

[8] T. W. Lian, A. Kondo, T. Kozawa, T. Ohmura, W. H. Tuan, M. Naito, Ceramics International 41 (2015) 9966-9971.

[9] H. Abe, I. Abe, K. Sato, M. Naito, Journal of the American Ceramic Society 88 (2005) 1359-1361.

[10] I. Abe, K. Sato, H. Abe, M. Naito, Advanced Powder Technology 19 (2008) 311-320.

[11] M. Naito, A. Kondo, T. Yokoyama, ISIJ International 33 (1993) 915-924.

[12] J. A. Cape, G. W. Lehman, Journal of Applied Physics 34 (1963) 1909-1913.

[13] M. Akoshima, B. Hay, M. Neda, M. Grelard, International Journal of Thermophysics 34 (2013) 778-791.

[14] Y-G. Kwon, S-Y. Choi, E-S. Kang, S-S. Beak, Journal of Materials Science 35

(2000) 6075-6079.

[15] D. Tahara, Y. Itoh, T. Ohmura, H. Abe, M. Naito, Ceramic Transactions 146 (2004) 173-177.

[16] T. W. Lian, A. Kondo, M. Akoshima, H. Abe, T. Ohmura, W. H. Tuan, M. Naito, Advanced Powder Technology 27 (2016) 882-885.

[17] Technical Bulletin 11: Basic Characteristics of AEROSILR Fumed Silica, EVONIK INDUSTRIES. (2006).

[18] J. Mathis, G. Wannemacher, Journal of Colloid and Interface Science 125 (1988) 61-68.

Chapter 4

Effect of Mechanical Processing on Thermal and Mechanical Properties of Fibrous Alumina Compacts

Abstract

In the first part of this chapter, a method to measure the thermal conductivity of specimens is proposed. An apparatus with simple structure has been developed. The thermal conductivity of porous compact board is measured by this method. The result of thermal conductivity shows good agreement for that obtained by the cyclic heat method. The second part of this chapter aims at developing a fibrous alumina compact which is available at higher temperature thermal insulation. In Chapter 2 and Chapter 3, we have used fumed silica/glass fiber to prepare the thermal insulation compact. However, the silica particle and glass fiber are not suitable for high temperature (> 600 °C). Present section prepares the thermal insulation by using the fumed alumina nanoparticle and alumina fiber. The prepared compact is expected to have nanoporous structure similar to that introduced in Chapter 2. Also, the mechanical processing parameters to make the composite fibers by using them are examined. The thermal conductivity is measured by the method explained in first part. The thermal conductivity of the compact is as low as 0.036 W/m·K. With the increase of rotating speed, the thermal conductivity increases to around 0.042 W/m·K. The strength decreases with the increase of processing time. Therefore, a lower rotating speed and a shorter processing time are favorable. The thermal and mechanical properties can be related to the surface structure of processed alumina fibers and formation of granules of alumina nanoparticles.

4.1 The development of measuring method of thermal conductivity

4.1.1 Introduction and background

Recently, the problems of global warming and energy shortage are becoming serious issues facing the world. To insulate the thermal energy from the heat source is thus an important issue. For the solution, the development of high performance thermal insulation material is needed. Due to the thermal conductivity is an index for thermal insulation ability, measuring it more precisely plays an important role in such developing process. For measuring the thermal conductivity of thermal insulations, the GHP method (belongs to steady-state method) is widely used.

In thermal conductivity measurement apparatus based on steady-state method, uniform temperature gradient in the test specimen must be achieved for applying Fourier’s low. However, complicated apparatus structure is needed for satisfying such condition. For instance, in GHP method [1], the heater contacting the high temperature side of specimen must have the separated structure of main hot plate and guarded hot plate. Such structure contributes to keeping the uniform temperature gradient of specific region in the specimen. However, it results in the complicated apparatus structure and complicated temperature controlling process. Therefore, the measuring apparatus is generally very expensive. This section proposes a method to determine the thermal conductivity of specimens with ununiformed temperature gradient region. It makes use of apparatus with simple structure.

4.1.2 Measuring method of thermal conductivity

Figure 4.1 shows the cross section of the measurement system. The temperature of Heater 2 is controlled to keep the temperature of Heater 1 equal to Heater 2 ($\theta_{h1} = \theta_{h2}$). Thus, all the amount of heat, Q, generated at the Heater 1 flowed in the specimen is supposed. In addition, the amount of heat, Q, is supposed to be the sum of (i) the amount of heat in thickness direction, Q_t, and (ii) the amount of heat loss from specimen and heaters, Q_{loss}, as shown in the equation below:

$$Q = Q_t + Q_{loss} \tag{4.1}$$

Here, the amount of heat in thickness direction, Q_t, is supposed to follow the Fourier's low as well, as shown in below:

$$Q_t = \lambda_t \frac{\Delta\theta}{d} S \tag{4.2}$$

In above equation, d is the thickness of specimen, Q_t the amount of heat in thickness direction, S the heat flow area, $\Delta\theta$ the differential temperature in thickness direction (= θ_{h1} - θ_{h3}), λ_t the thermal conductivity in thickness direction of specimen.

On the other hand, for the amount of heat from Heater 1 flowed into the specimen, Q, the following of the Fourier's low is also supposed. Thus, Q is supposed to the direct proportion to the temperature gradient, $\Delta\theta/d$, and heat flow area, S; and has the coefficient, λ_c. Therefore, Q can be shown as below:

$$Q = \lambda_c \frac{\Delta\theta}{d} S \tag{4.3}$$

In addition, if the differential temperature in plane direction, $\Delta\theta_{loss}$, is supposed; the amount of heat loss from specimen and heaters, Q_{loss}, can be represented by the multiplication of thermal conductance in the plane direction of specimen, H, and $\Delta\theta_{loss}$, as shown in below:

$$Q_{loss} = H \cdot \Delta\theta_{loss} \tag{4.4}$$

Then, the following equation is obtained by assigning the Eq. (4.2) - Eq. (4.4) to Eq. (4.1):

$$\lambda_c = \lambda_t + a \cdot \Theta \tag{4.5}$$

Here, the coefficient a and dimensionless temperature Θ are represented by the following Eq. (4.6) and Eq. (4.7), respectively:

$$a = \frac{H \cdot d}{S} \tag{4.6}$$

$$\Theta = \frac{\Delta\theta_{loss}}{\Delta\theta} \tag{4.7}$$

As represented in Eq. (4.5), the dimensionless temperature Θ has linear relationship with the coefficient λ_c. In present method, $\Delta\theta$ is changed several times to determine the coefficient λ_c in Eq. (4.3). $\Delta\theta_{loss}$ is determined from the temperature distribution on specimen's surface at that time. Thus the Θ is obtained from Eq. (4.7). Then, the linear relationship between Θ and λ_c is plotted as shown in Fig. 4.2. Therefore, the thermal conductivity in thickness direction of specimen, λ_t, is represented by the intercept.

In present method, the temperature distribution at high temperature surface of specimen (between Heater 1 and specimen in Fig. 4.1) is measured. The θ_{hm} is obtained from the temperature distribution which is measured from the origin set at the center to the edge, as shown in Fig. 4.1. Then, the differential temperature, $\Delta\theta_{loss}$, is determined from the difference of θ_{hm} and θ_{h1} (temperature at the center of high temperature surface of specimen), as shown in below:

$$\Delta\theta_{loss} = \theta_{h1} - \theta_{hm} \tag{4.8}$$

Further details for the measuring method can be found elsewhere [2].

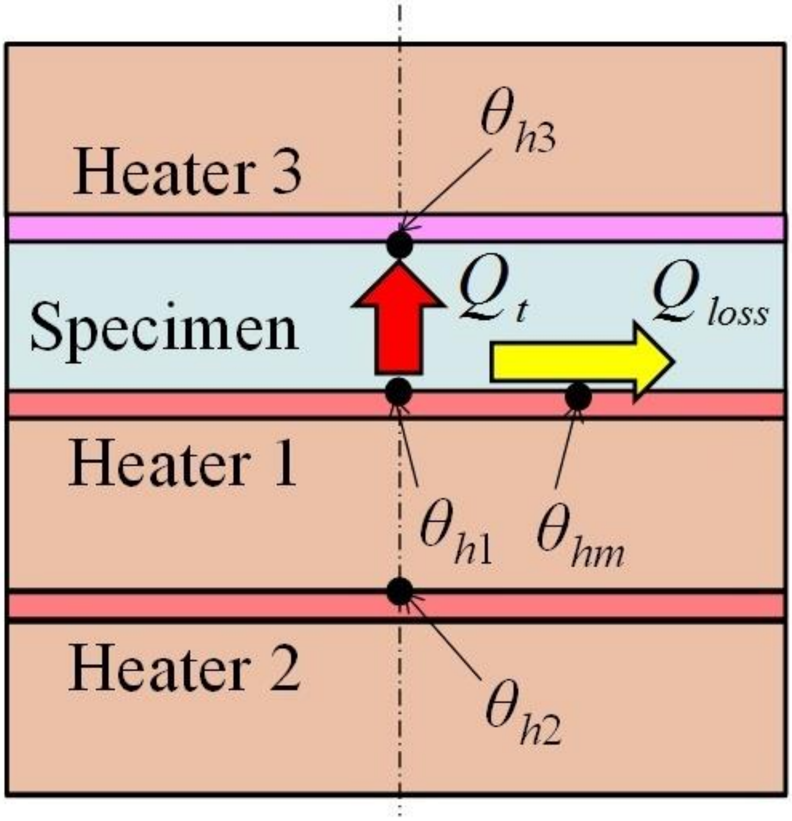

Fig. 4.1 Cross section of the measurement system.

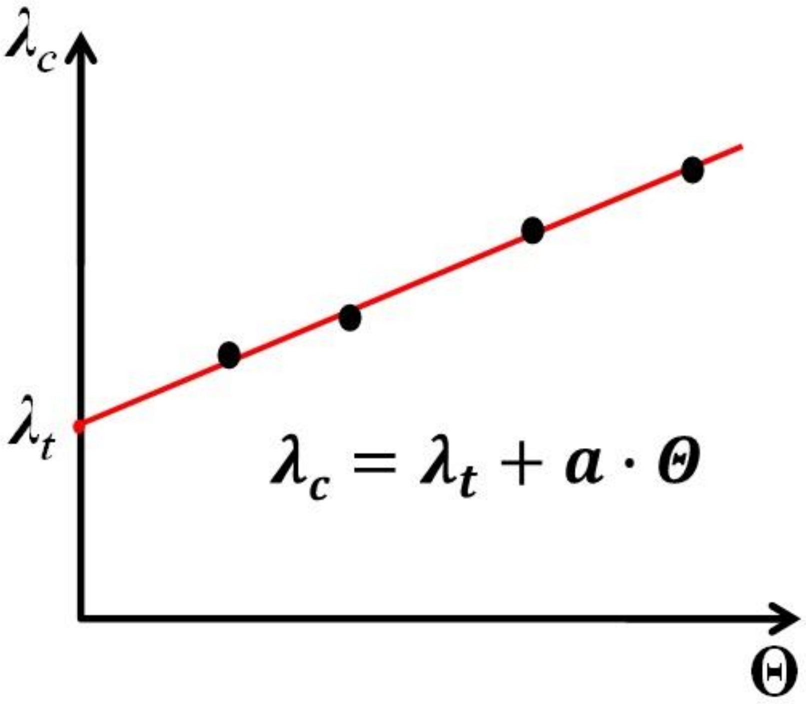

Fig. 4.2 Image of the determination of thermal conductivity by proposed method.

4.1.3 Developed measuring apparatus

Figure 4.3 shows the schematic image of the measurement system. The system consists of the following devices: Heater 1 controlled by Temperature controller 1, heats one side of specimen. Heater 3 voltaged by Variable transformer, heats another side of specimen. Heater 2 controlled by Temperature controller 2, prevents the heat energy (generated by Heater 1) flowing to opposite side of specimen (downward direction in Fig. 4.3). Digital multi-meter reads the output voltage of Heater 1. Recorder records the temperature of each part of the specimen.

Figure 4.4 shows the measuring part of the apparatus. Heater 1 and Heater 2 are the same ceramics heater. The thickness is around 50 mm. Heater 3 consists of 2 pieces of 1 mm thickness rubber heaters. There is a calcium silicate insulation set on Heater 3. Two boards of polystyrene form with 20 mm thickness are set under Heater 2. The size of specimen is about 300 mm × 300 mm. The feasible thickness of specimen for the measurement is around 10 mm ~ 50 mm.

Figure 4.5 shows the positions of thermocouples. Points of × sign in the figure shows the positions of set thermocouples. Viewing direction of the figure is from the top view of the measurement system in Fig. 4.1. The thermal couple at interface between Heater 2 and polystyrene form is set as shown in Fig. 4.5 (a). The thermal couples at high temperature surface of specimen (between Heater 1 and specimen), low temperature surface of specimen (between Heater 3 and specimen), and the interface between Heater 1 and Heater 2 are set as shown in Fig. 4.5 (b).

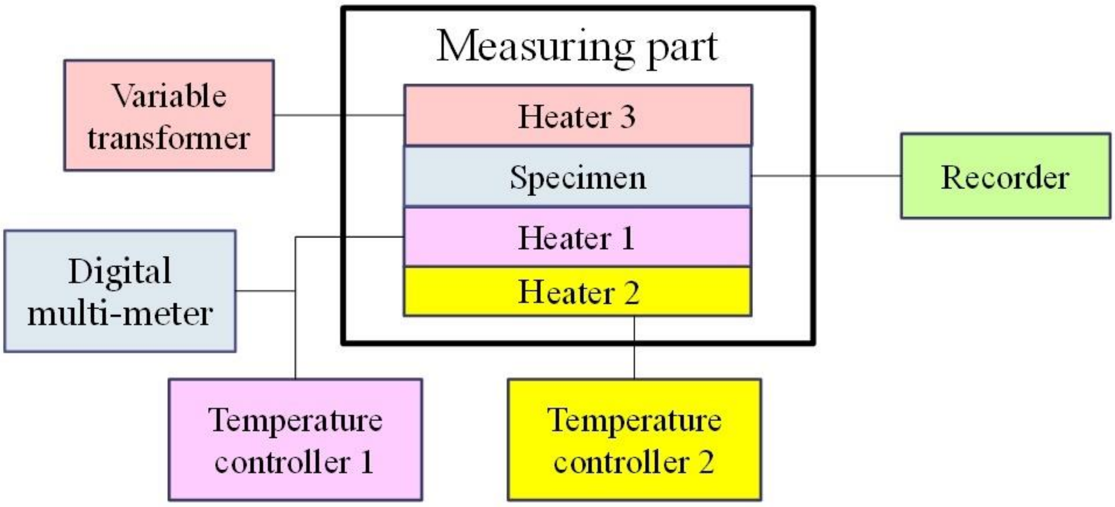

Fig. 4.3 Schematic diagram of the measurement system.

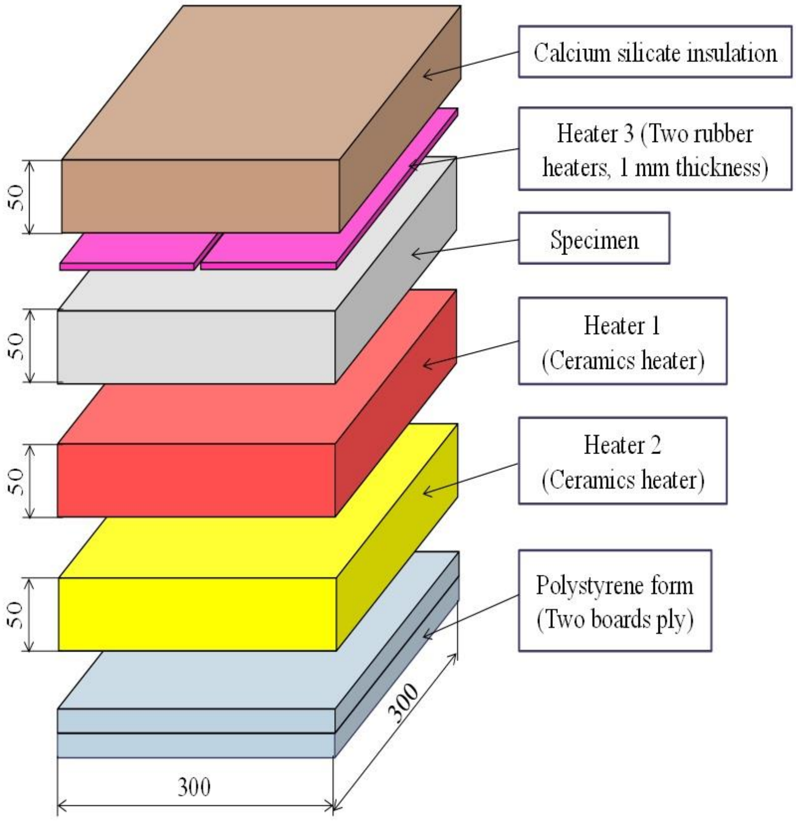

Fig. 4.4 Measurement part of the apparatus.

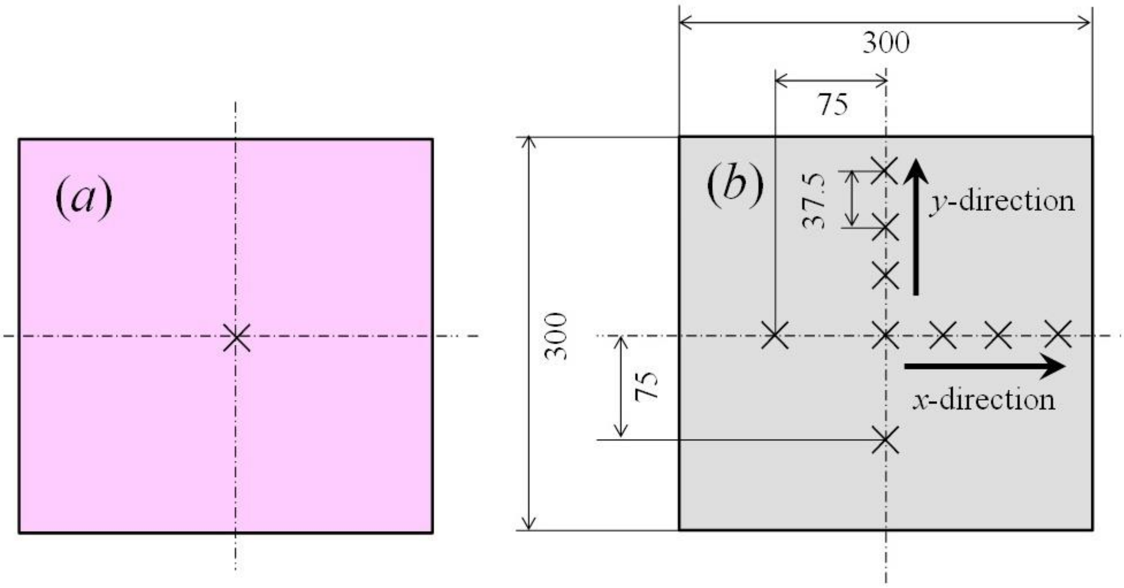

Fig. 4.5 Positions of thermocouples.

4.1.4 Information of test specimen

The preparation process of the test specimen was almost the same as mentioned in section 2.2.1. The sources of starting materials were different. Brief information is given here. The starting materials were hydrophilic fumed silica powder (AEROSIL300, Nippon Aerosil, Tokyo, Japan), glass fiber (CS3J-891, Nittobo, Tokyo, Japan) and SiC powder (GMF-6S; Pacific Rundum, Toyama, Japan). The length and diameter of the fiber were 3 mm and 10 μm, respectively. The specific surface area of the SiC powder was 5.4 m^2/g. The average diameter of SiC was 1.9 μm. The ratio (mass%) of fumed silica: glass fibers: SiC in the powder mixture was 60:20:20. The average density of the prepared specimen was around 390 kg/m^3.

4.1.5 Reliability of the developed measuring method of thermal conductivity

Figure 4.6 shows the result of thermal conductivity measurement of test specimen. The circle mark indicates the results of the proposed method and the square mark indicates the results measured by cyclic heat method (the same meaning as periodic heat method) [3,4]. As shown in Fig. 4.6, the results of different measuring methods exhibited good agreement. It means the proposed method is reliable for measuring the thermal conductivity.

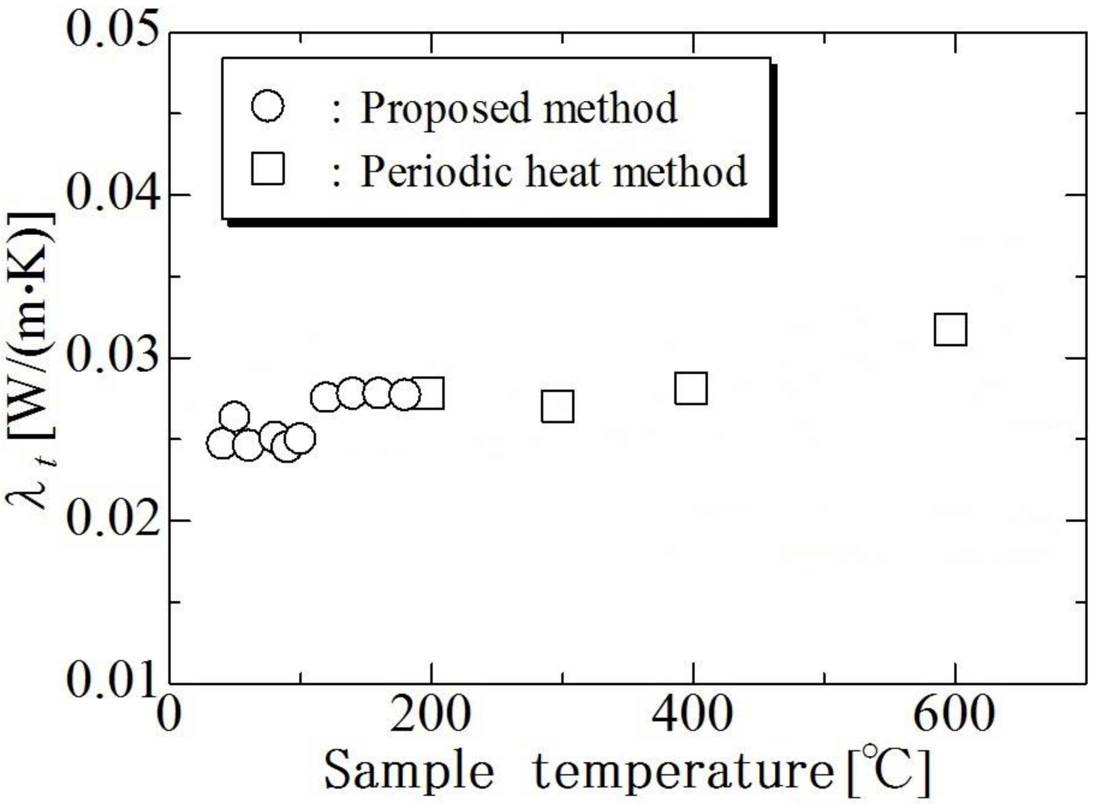

Fig. 4.6 Thermal conductivity of fibrous fumed silica compact measured by proposed method and conventional method.

4.2 Effect of mechanical processing on the thermal and mechanical properties of fibrous fumed alumina compacts

4.2.1 Introduction

In recent year, fast industrial growth and large energy usage induces harsh environmental problems [5-7]. Particularly, the problems can be related to the waste heat generated from factories, industrial furnaces, buildings and houses. Thus, to reduce the waste heat efficiently is an important subject.

Developing a high performance thermal insulation material is one of the solutions. The ceramic compacts with porous structure, especially nanoporous structure, are preferred for such thermal insulations [8-10]. As explained in Chapter 2 and Chapter 3, the glass fiber reinforced silica nanoporous compacts have been successfully prepared using mechanical processing method [3,11-14]. An extremely low thermal conductivity around 0.026 W/m·K (at 100 °C) is obtained [11,12] by combining cyclic heat method [15-17] and drop calorimeter method [18]. The compacts can be used as the advanced thermal insulation materials. But, due to the silica nanoparticles (both hydrophilic and hydrophobic) and glass fibers are unstable at high temperature range [19,20], the applications of such silica compacts above 600 °C are difficult. Therefore, for the high temperature applications, alternative fibrous ceramic compacts are needed.

As the melting point of alumina is higher than that of silica, the use of alumina may improve the insulation capability at high temperature. Though a lot of attention has been given to the use of alumina nanoparticles for engineering purposes, its application for thermal insulation is still lacking [4]. Present section aims to develop a compact composing of ceramic fiber and fumed alumina particles. The starting materials are hydrophilic surface type fumed alumina nanoparticles, ceramic fibers and SiC powders. The length of ceramic fiber is in several centimeters; the alumina content is as high as 80%. It is expected to have similar nanoporous structure as hydrophilic type silica compact showed in Chapter 2.

The previous study [12] pointed out that the property of the porous ceramic compact may be affected by the mechanical processing parameters. Therefore, present study focuses on the evaluation of mechanical processing parameters on the thermal conductivity and strength of the fibrous alumina compacts. Two important processing parameters, rotating speed and processing time, are evaluated. The thermal conductivity measurement was conducted in the temperature from 100 °C to 350 °C. The strength of the compacts was also measured. The microstructure characteristics of porous thermal insulation compact are also evaluated.

4.2.2 Experimental procedure

(1) Sample preparation

The starting materials were fumed alumina powder (AEROXIDE®Alu130; Nippon Aerosil, Tokyo, Japan), ceramic fibers (B80, DENKA ALCEN; 80% Al_2O_3 and 20% SiO_2, Denka, Tokyo, Japan) and SiC powder (GMF-6S; Pacific Rundum, Toyama, Japan). The specific surface area of the fumed alumina was 128 m^2/g, as determined by a BET method (3Flex Surface Characterization Analyzer, Micromeritics Japan, Chiba, Japan). The equivalent size of alumina nanoparticle was 12 nm, as calculated from the surface area.

The micrograph of the starting fibers is shown in Fig. 4.7 (a). The addition of ceramic fibers might enhance the strength and thermal resistance of the resulting insulation compact [4]. The diameter and length of the fibers were around 4 μm and several centimeters, respectively. Since the melting point of alumina is higher than that of silica, the thermal stability of used ceramic fiber would be better than that of glass fiber. The SiC was added to control the radiation heat transfer of the compact. The specific surface area of the SiC powder was 5.4 m^2/g. The average diameter of SiC was 1.9 μm, as determined by a particle size analyzer (Microtrac MT3300 EXII, NIKKISO, Tokyo, Japan). Fig. 4.7 (b) shows the morphology of starting SiC particles observed by scanning electron microscopy (SEM, JSM-6010LA, JEOL Ltd., Tokyo, Japan).

The composition of the starting powder mixtures is shown in Table 4.1. The compounding ratio (%) of fumed alumina: ceramic fibers: SiC powder in the powder mixture was 65: 20: 15. For each batch, 100 g powder mixture was used. The starting mixtures were treated by the mechanical processing method, using the horizontal axis type shearing mixer (Hosokawa Micron Corp., Osaka, Japan) [21], as shown in Fig. 1.2. The effect of following processing parameters was evaluated: (1) the rotating speed and (2) the processing time. The rotating speed was set at 1000 rpm, 1500 rpm and 2000 rpm; the processing time was set at 1 min, 5 min and 10 min, respectively. The temperature and humidity of atmosphere during the processing were set around 300 K and 50%, respectively. The processed powder mixture (fumed alumina/ceramic fiber/SiC) was obtained after the mechanical processing. The morphology of the processed powders was observed by SEM. And the specific surface area of the processed powders was determined by the BET method. Then, the processed powder was put in a square die and pressed uniaxially to form the board (100 mm × 150 mm × 10 mm), by using a uniaxial pressure of 2 MPa. The apparent density and porosity of the compact board were determined by measuring its dimensions and weight.

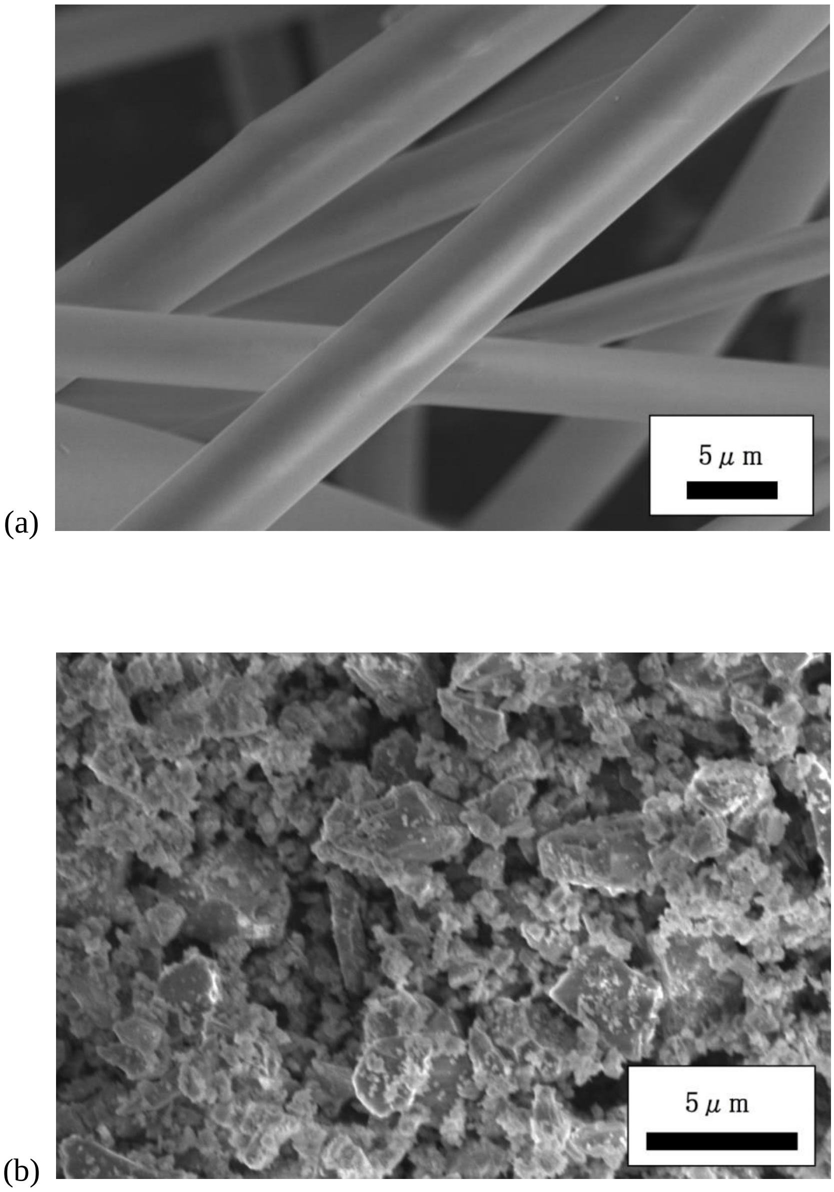

Fig. 4.7 SEM image of starting (a) ceramic fibers and (b) SiC particles.

Table 4.1 Composition of the fibrous alumina compacts prepared in the present study.

Material	Compounding ratio	Average diameter
Alumina nanoparticle	65 mass%	12 nm
Ceramic fiber	20 mass%	4 μm (length: several cm)
SiC particle	15 mass%	1.9 μm

(2) Sample characterizations

In this study, the thermal conductivity was measured by the method proposed in section 4.1 [2]. The measuring temperatures varied from 100 °C to 350 °C. The details for the method and measuring apparatus can be found in section 4.1 [2]. The strength measurement was conducted by a three-point bending test, using a universal testing machine. The dimensions of the specimens were 100 mm × 30 mm × 10 mm, prepared from the compact. The span was 80 mm; the crosshead speed was 1 mm/min. For the specimens prepared by each processing condition, 3 specimens were measured. After measuring the fracture load, the flexural strength was determined.

4.2.3 Results

(1) Characterization of processed powder mixtures

Figure 4.8 (a) - (e) shows the morphology of the ceramic fibers after the mechanical processing with different processing parameters. The fibers are well-coated with a surface layer composing of alumina nanoparticles. With the processing time of 1 min, the fiber prepared with the highest rotating speed (2000 rpm) shows a thick surface layer, as demonstrated in Fig. 4.8 (c). From Fig. 4.8 (a) - (c), the thickness of surface layer increases roughly with increasing the rotating speed. On the other hand, at a constant rotating speed of 1000 rpm, the thickness of surface layer on fibers is almost the same, as shown in Fig. 4.8 (a), (d) and (e).

Figure 4.9 (a) - (c) shows the SEM images of the alumina particles dispersed in the processed powder with different processing parameters. The images were obtained by observing the processed powder set on the sample holder, and controlling the field of view on the area except fibers. From Fig. 4.9 (c), large and porous granules of alumina nanoparticles around several tens of micrometers are observed with the processing parameter of 10 min / 1000 rpm. The morphology of the particles is almost similar as the powder mixture treated with 1 min / 1000 rpm and 1 min / 2000 rpm, as shown in Fig. 4.9 (a) and (b). From the figures, it indicates that the alumina granule size is affected by the processing time, which may underline the properties of the resulted compact.

Figure 4.10 (a) and (b) shows the relationships between the specific surface area (SSA) of processed powder as a function of the processing parameters. With the increase of rotating speed, the SSA decreases from 95 m^2/g to around 60 m^2/g. With the increase of processing time, the SSA also decreases but slightly from 95 m^2/g to around 80 m^2/g. The decrease of SSA in both figures referred to the forming of composite particles after the mechanical processing. The large decrease of SSA in higher rotating speed condition may be due to the densely packed structure of nanoparticles on fiber surface as shown in Fig. 4.8 (c).

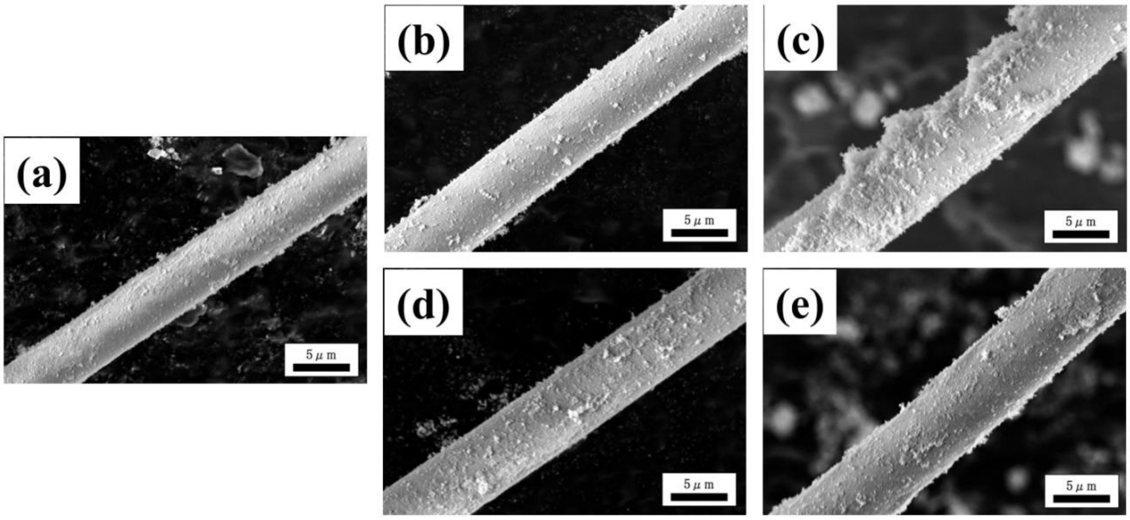

Fig. 4.8 Coated ceramic fibers processed for the time / speed of (a) 1 min / 1000 rpm, (b) 1 min / 1500 rpm, (c) 1 min / 2000 rpm, (d) 5 min / 1000 rpm, and (e) 10 min / 1000 rpm.

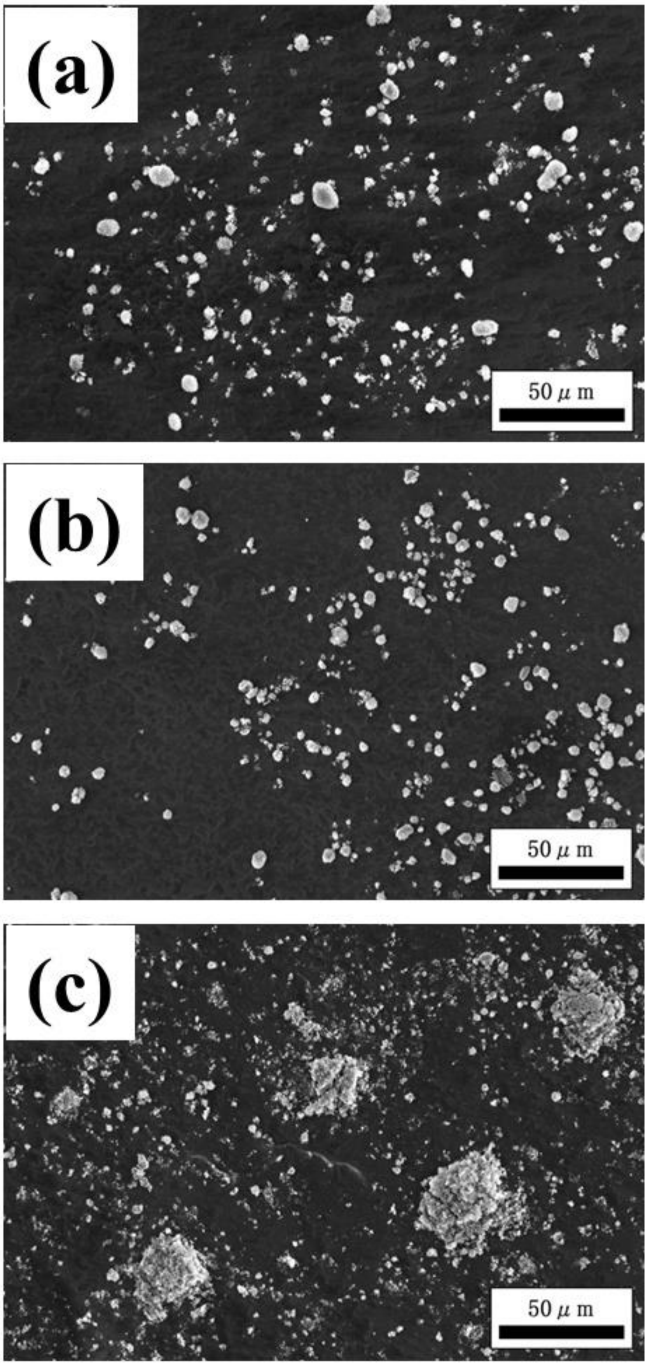

Fig. 4.9 Dispersed alumina particles processed for time / speed of (a) 1 min / 1000 rpm, (b) 1 min / 2000 rpm, and (c) 10 min / 1000 rpm.

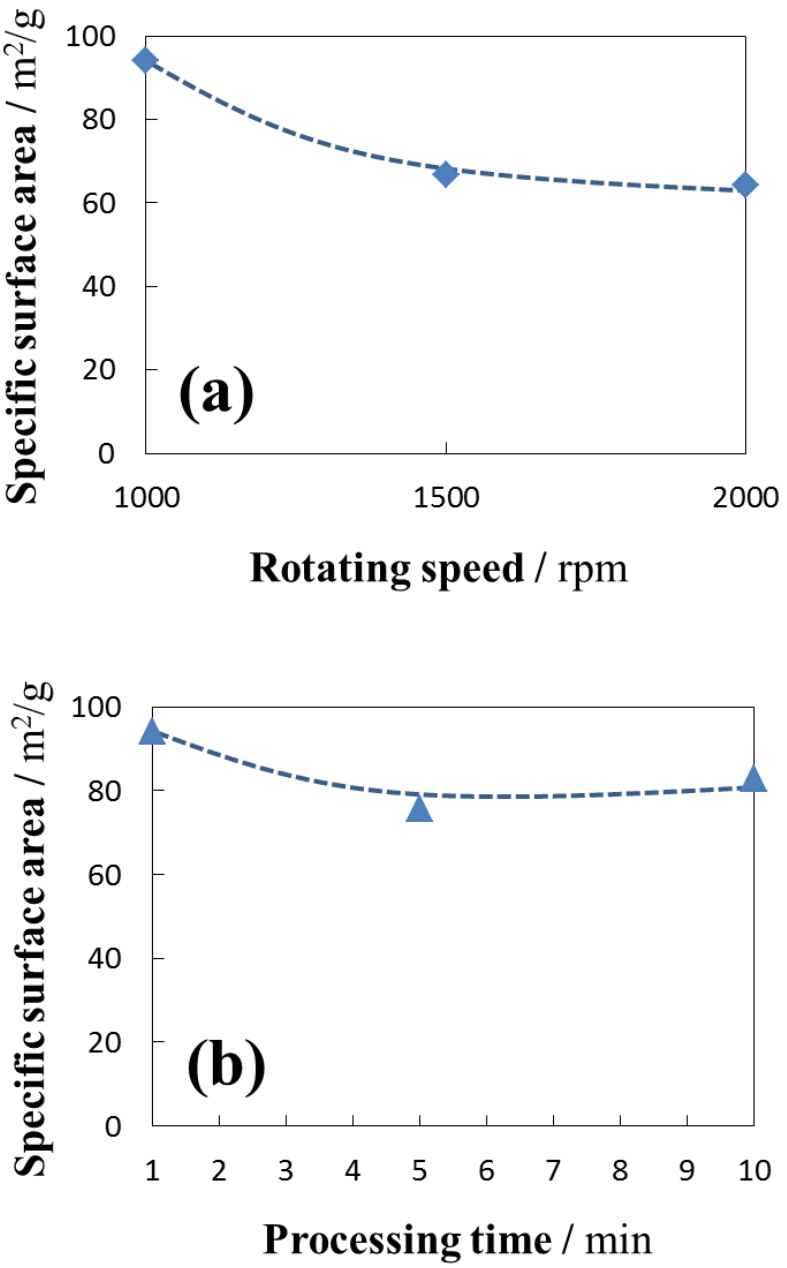

Fig. 4.10 Specific surface area of the powders processed (a) for 1 min at various speeds and (b) at 1000 rpm for various processing times.

(2) Characterization of fibrous alumina compact

Table 4.2 shows the values of apparent density and porosity of the fibrous alumina compacts with different processing parameters. The table indicates that the fibrous fumed alumina compacts with high porosity and light weight are successfully prepared.

The thermal conductivity of the compacts processed with 3 different parameters is shown in Fig. 4.11. Within the temperature range measured (100 °C to 350 °C), the fibrous compact processed at 1000 rpm for 1 min shows the lowest thermal conductivity, around 0.036 W/m·K. However, the thermal conductivity increases to 0.042 W/m·K as the rotating speed increases to 2000 rpm. The compact treated at 1000 rpm for 10 min also exhibits a low thermal conductivity of 0.037 W/m·K. Fig. 4.11 suggests that the rotating speed is an important parameter in terms of thermal conductivity.

Figure 4.12 shows the strength for the fibrous compact. Error bar in the figure indicates one standard deviation. The strength of the compact treated at 1000 rpm for 1 min is 0.58 MPa. The value is high enough to allow the subsequent machining on the fibrous compact. From the figures, it is observed that the strength drops with the increase of processing time.

Table 4.2 Density and porosity of fibrous alumina compacts with various processing parameters.

Processing time (min)	Rotating speed (rpm)	Apparent density (kg/m³)	Porosity (%)
1	1000	538	85.5
1	1500	554	85.1
1	2000	603	83.8
5	1000	583	84.3
10	1000	585	84.3

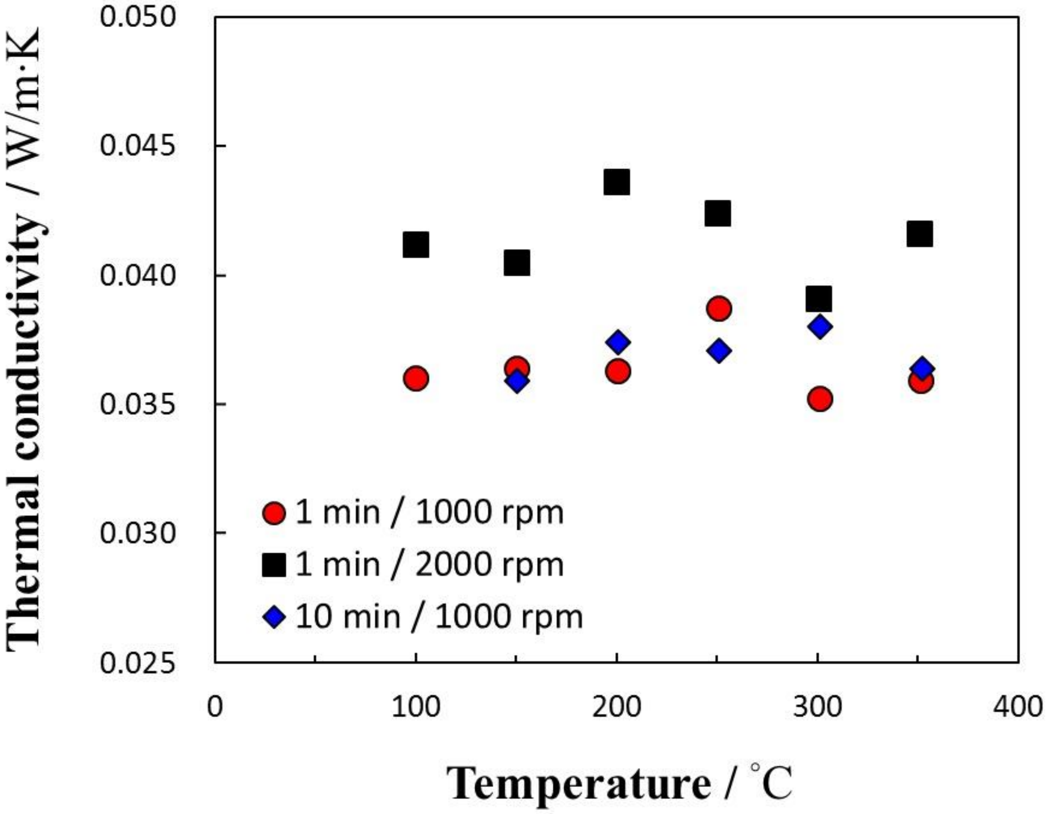

Fig. 4.11 Thermal conductivity of fibrous alumina compacts after processing for the time / speed of 1 min / 1000 rpm, 1 min / 2000 rpm, and 10 min / 1000 rpm.

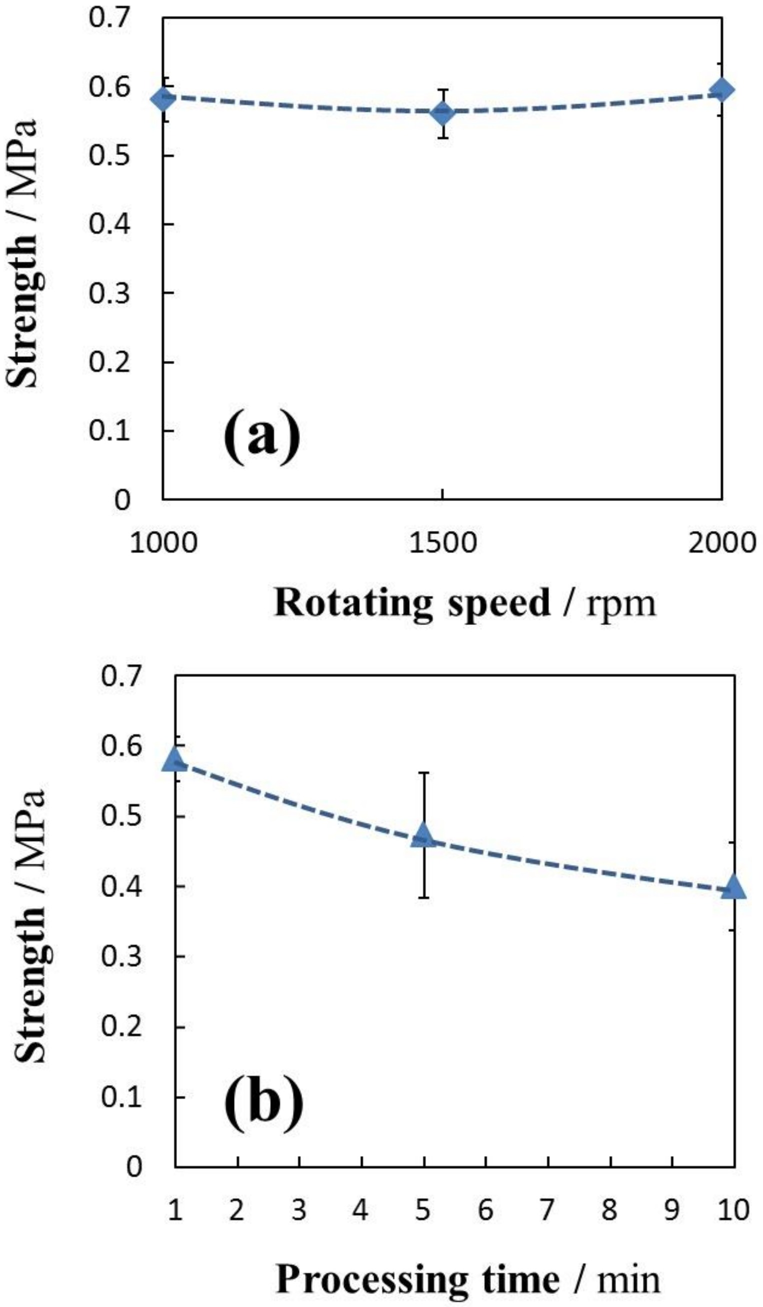

Fig. 4.12 Strength of the fibrous alumina compacts processed (a) for 1 min at various speeds and (b) at 1000 rpm for various processing times.

(3) Fabricated alumina compact for high temperature thermal insulation

The fumed alumina nanoparticles are expected as a relatively stable material for high temperature [22], comparing with that of the fumed silica as explained in Chapter 2 [20]. Therefore, the relationship between the volume shrinkage and heat treatment temperature of thermal insulations made of them was investigated. The specimens of fibrous fumed silica compact (glass fiber used, the composition is close to the samples used in Chapter 2 and 3 [23]) and fibrous fumed alumina compact (processing parameters of (1min, 1000 rpm) in this study) were heat treated. The dwelling time was 1 hour. The results are shown in Fig. 4.13 (a) and (b). In Fig. 4.13 (a), the volume shrinkage of silica specimen started to increase at the temperature of 550 °C. The value finally reached around 3% with heat treated in 750 °C. On the other hand, as in Fig. 4.13 (b), the volume shrinkage of alumina specimen was around -0.5% ~ +0.5% at the heat treated temperature range from 800 °C to 1100 °C. The change of volume was very slightly and was almost in the range of measuring error. Therefore, the fibrous fumed alumina compacts prepared in present study have the possibility to be applied as the thermal insulation material for high temperature.

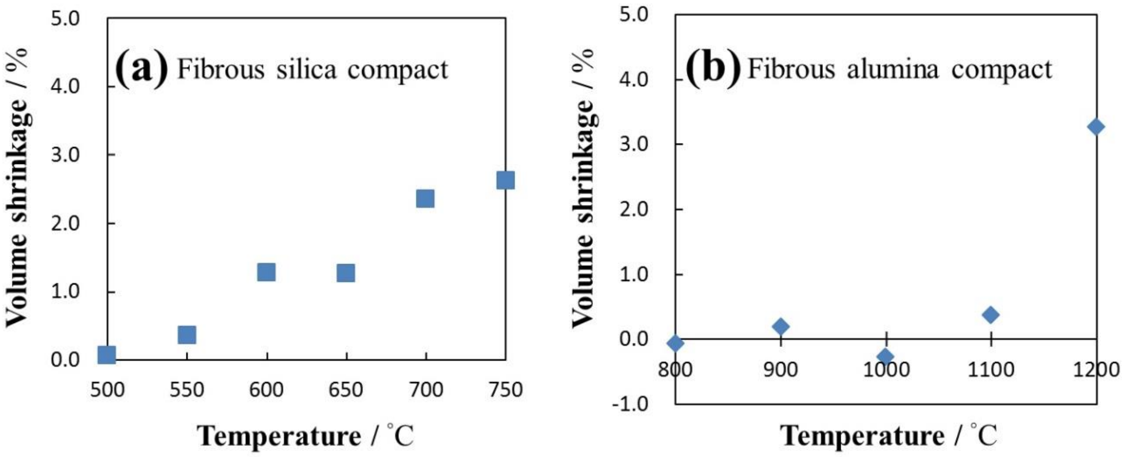

Fig. 4.13 The volume shrinkage of (a) fibrous silica compact (glass fiber) and (b) fibrous alumina compact (ceramic fiber) with heat treated at high temperature.

4.2.4 Discussion

After the mechanical processing, all fibers are well-coated with alumina nanoparticles (Fig. 4.8). It indicates that the direct contacts between fiber and fiber in the compact are hindered by the presence of alumina surface layer. In addition, since the nanoparticles are bonded on the surface of fibers, a uniform dispersion of ceramic fibers within alumina nanoparticles can be achieved. Therefore, it is possible to manipulate the heat transfer within the fibrous compact with a high loading amount of fibers. The thermal conductivity of the compact is thus controlled by the alumina nanoparticle layer, despite the fiber content is high. The thermal conductivity of the fibrous alumina compact keeps low till a temperature of 350 °C. It will be of interest to investigate its thermal stability at a temperature higher than 350 °C.

The compact shows a relatively high thermal conductivity as the powder is processed at 2000 rpm for 1 min, as shown in Fig. 4.11. According to Fig. 4.8 (c), the coated alumina layer on the fiber is thick. Such particle morphology may increase the contact areas between coated fiber and other particles, adding to the increase of apparent density of the compact (Table 4.2). It leads to the increasing solid conduction of heat transfer. On the other hand, the thermal conductivity of the compact with the fiber treated with 1 min / 1000 rpm and 10 min / 1000 rpm is low. For these compacts, the coated layer is thin. Their morphology is similar, as shown in Fig. 4.8 (a), (d) and (e).

In Fig. 4.12, the strength almost does not change with the increase of rotating speed. However, the strength drops with the increase of processing time. The increase of processing time affects the size of alumina granules, as demonstrated in Fig. 4.9. The larger size of granules induces less contact point between particles in resulted compact. A longer processing time thus leads to a lower strength.

4.3 Conclusions

(1) A method to measure the thermal conductivity of specimens is proposed.

(2) The effect of mechanical processing conditions on the thermal and mechanical properties of fibrous alumina compact was investigated. The thermal conductivity of the fibrous compact was as low as 0.036 W/m·K. The thermal conductivity kept low with up to 350 °C.

(3) With the increase of rotating speed, the thermal conductivity increased to around 0.042 W/m·K. On the other hand, the strength decreased with the increase of processing time.

(4) A lower rotating speed and a shorter processing time are favorable for better performance of the compact.

(5) The thermal and mechanical properties can be related to the surface structure of coated alumina fibers and the formation of granules of alumina nanoparticles.

References

[1] JIS A 1412-1.

[2] T. Ohmura, T. W. Lian, A. Kondo, R. Hayasaka, M. Naito, Netsu Bussei 31 (2017) 166-173.

[3] T. Ohmura, I. Abe, Y. Ito, K. Sato, H. Abe, M. Naito, Journal of the Society of Powder Technology, Japan 46 (2009) 461-466.

[4] T. Ohmura, Y. Ito, I. Abe, H. Abe, M. Naito, Journal of the Society of Powder Technology, Japan 46 (2009) 806-812.

[5] A. B. Stambouli, E. Traversa, Renewable and Sustainable Energy Reviews 6 (2002) 433-455.

[6] I. Dincer, M. A. Rosen, International Journal of Energy Research 22 (1998) 1305-1321.

[7] L. Lombard, J. Ortiz, C. Pout, Energy and Buildings 40 (2008) 394-398.

[8] M. Reim, W. Korner, J. Manara, S. Korder, M. Arduini-Schuster, H. P. Ebert, J. Fricke, Solar Energy 79 (2005) 131-139.

[9] G. S. Wei, Y. S. Liu, X. X. Zhang, F. Yu, X. Z. Du, International Journal of Heat and Mass Transfer 54 (2011) 2355-2366.

[10] T. W. Clyne, I. O. Golosnoy, J. C. Tan, A. E. Markaki, Philosophical Transactions of the Royal Society A: Mathematical, Physical and Engineering Sciences 364 (2006) 125-146.

[11] H. Abe, I. Abe, K. Sato, M. Naito, Journal of the American Ceramic Society 88 (2005) 1359-1361.

[12] I. Abe, K. Sato, H. Abe, M. Naito, Advanced Powder Technology 19 (2008)

311-320.

[13] T. W. Lian, A. Kondo, T. Kozawa, T. Ohmura, W. H. Tuan, M. Naito, Ceramics International 41 (2015) 9966-9971.

[14] T. W. Lian, A. Kondo, T. Kozawa, M. Akoshima, H. Abe, T. Ohmura, W. H. Tuan, M. Naito, Journal of Asian Ceramic Societies 5 (2017) 118-122.

[15] H.S. Carslaw, J. C. Jaeger, Oxford University Press, New York (1959).

[16] T. Ohmura, M. Tsuboi, Netsu Bussei 13 (1999) 264-270.

[17] T. Ohmura, M. Tsuboi, M. Onodera, T. Tomimura, Thermal Science and Engineering 11 (2003) 43-44.

[18] T. Ohmura, M. Tsuboi, M. Onodera, T. Tomimura, International Journal of Thermophysics 24 (2003) 559-575.

[19] J. B. Lasky, Applied Physics Letters 48 (1986) 78-80.

[20] J. Mathis, G. Wannemacher, Journal of Colloid and Interface Science 125 (1988) 61-68.

[21] M. Naito, A. Kondo, T. Yokoyama, ISIJ International 33 (1993) 915-924.

[22] M. I. F. Macêdo, C. A. Bertran, C. C. Osawa, Journal of Materials Science 42 (2007) 2830-2836.

[23] T. W. Lian, A. Kondo, M. Akoshima, H. Abe, T. Ohmura, W. H. Tuan, M. Naito, Advanced Powder Technology 27 (2016) 882-885.

Chapter 5

Conclusions

In this study, nanoporous materials prepared by mechanical method for thermal insulation were selected, and their promising producing conditions were discussed. The compounding of starting materials and the mechanical processing parameters were mainly investigated. In Chapter 2, the effect of particle surface properties, hydrophilic or hydrophobic of silica particles, on the thermal property of the resulted compact was investigated. Based on the result of Chapter 2, in Chapter 3, the effect of addition ratio of hydrophobic silica to hydrophilic silica on the thermal and mechanical property of the fibrous silica compacts was investigated. In Chapter 4, for the high temperature thermal insulation, fibrous alumina compacts were prepared. Besides, the effects of processing parameters of processing time and rotating speed on the properties of the compact were investigated. The main conclusions are summarized as follows:

In Chapter 1, the background of this study and its objectives were explained.

In Chapter 2, the effect of the hydrophilic or hydrophobic surface structure of fumed silica particles on the thermal conductivity and mechanical strength of the resultant compact board was investigated. It was found that the thermal conductivity and strength of the compact boards were affected by the characteristics of used silica particles. Higher thermal conductivity and higher strength were obtained for the compact using hydrophilic silica. Lower thermal conductivity and lower strength were obtained for the compact using hydrophobic type. The difference of thermal conductivity was mainly resulted from the heat transfer between solid parts. The Si-O bonding between particles played an important role. The difference of strength was resulted from the bonding between fiber-silica and that between silica-silica particles.

In the first part of Chapter 3, a rapid measurement of the thermal diffusivity of porous thermal insulation material by laser flash method was proposed. The specific heat capacity was determined by DSC method. Thermal conductivity was obtained from the results of density, thermal diffusivity, and specific heat capacity. Thermal conductivity of the nanoporous test specimen was 0.039 W/m·K, at room temperature. The thermal conductivities obtained by the laser flash method and DSC method exhibited good agreement with the data obtained by cyclic heat method. It suggested that the proposed method was very promising for rapid measurement of very low thermal conductivity materials.

In the second part of Chapter 3, the effect of addition ratio of hydrophobic silica to hydrophilic silica on the thermal conductivity and mechanical property of the fibrous silica compacts was investigated. The thermal conductivity was evaluated by the rapid measurement proposed in the first part of Chapter 3. It was found that with the addition of only 5% of hydrophobic silica particles, the thermal conductivity decreased from 0.042 W/m·K to 0.033 W/m·K; and decreased slightly with increasing the hydrophobic content up to 50%. The strength decreased with the addition of 5% hydrophobic silica; then decreased slightly with increasing the content from 10% to 50%. The change of thermal conductivity and strength was related to the coated surface structure of glass fiber in the resulted compact. With increasing hydrophobic silica content, the contacts between fiber and particles and the cohesive force between silica particles were decreased. Such tendency resulted in lower thermal conductivity and lower strength.

In the first part of Chapter 4, a method of measuring the thermal conductivity with the specimen was proposed. The apparatus could measure the specimen from room temperature up to 350 °C. The apparatus had relatively simple structure. Consequently, it was made clear that the thermal conductivity of fibrous fumed silica compact measured by this method showed good agreement with the results obtained from cyclic heat method.

The second part of Chapter 4, aimed at developing a fibrous fumed alumina compact board which was available at higher temperature. The effect of mechanical processing conditions on the thermal and mechanical properties of fibrous alumina compact was investigated. The thermal conductivity was evaluated by the method proposed in the first part of Chapter 4. The thermal conductivity of the fibrous compact achieved the low value of 0.036 W/m·K. The thermal conductivity kept low with the increase of measurement temperature up to 350 °C. With the increase of rotating speed, the thermal conductivity increased to around 0.042 W/m·K. The strength decreased with the increase of processing time. Therefore, a lower rotating speed and a shorter processing time were favorable for better performance of the compact. The thermal and mechanical properties could be related to the surface structure of coated alumina fibers and the formation of granules of alumina nanoparticles.

To sum up, in Chapter 2, it was made clear that tailored particle morphology such as glass fiber coated with nanoporous fumed silica layer was useful in thermal insulation compact. In Chapter 3, it was made clear that the resultant compact’s thermal conductivity and strength both decreased with increasing the hydrophobic type silica particle content. The balance of hydrophilic particle/hydrophobic particle in composition played an important role in compact’s properties. In Chapter 4, because the silica particle and glass fiber were not suitable for high temperature (> 600 °C), the hydrophilic type fumed alumina particle and alumina fibers were selected in preparing thermal insulation for high temperature use. With different purpose of usage, the thermal conductivity and strength of a compact could be designed based on above structure control concept.

In this doctoral dissertation, the structure control and characterization of nanoporous materials prepared by mechanical method were investigated. The application of the materials for thermal insulation field was also discussed. As a result, it is concluded that the present mechanical method is a promising one to prepare the high performance thermal insulation materials with green and energy-saving process. It is expected that present method has possibility to prepare more various functional materials with tailored nanostructure effectively. In the future work, further investigation of the preparing conditions for better performance of materials is needed. The improvement of the mechanical processing apparatus is also one of the important subjects.

Acknowledgement

This doctoral dissertation has been completed under the guidance of Professor Makio Naito of Joining and Welding Research Institute, Osaka University. I would like to express my gratitude to him for his valuable discussions and suggestions throughout this work.

I am grateful to Professor Yasufumi Fujiwara and Professor Tohru Sekino, of Division of Materials and Manufacturing Science, Graduate School of Engineering, Osaka University for their peer reviewing of the thesis.

I would like also to thank Professor Wei-Hsing Tuan, of Department of Materials Science and Engineering, National Taiwan University, Associate Professor Takahiro Ohmura, of Department of Intelligent Mechanical Engineering, National Institute of Technology, Wakayama College, Dr. Megumi Akoshima and Dr. Haruka Abe, of National Institute of Advanced Industrial Science and Technology, Associate Professor Hiroya Abe, Assistant Professor Takahiro Kozawa, Dr. Akira Kondo, of Joining and Welding Research Institute, Osaka University, for their valuable assistance.

I wish to express my appreciation to Japan-Taiwan Exchange Association for funding the doctor course of Engineering, Osaka University.

I wish to express my appreciation to all the members of Professor Naito's laboratory for their excellent contributions to this work.

I would like to express a special thanks to my parents and all my family for their continuous supports and encouragement.

List of publication

[1] T. W. Lian, A. Kondo, T. Kozawa, T. Ohmura, W. H. Tuan, M. Naito. Effect of Fumed Silica Properties on the Thermal Insulation Performance of Fibrous Compact, Ceramics International 41 (2015) 9966-9971.

[2] T. W. Lian, A. Kondo, M. Akoshima, H. Abe, T. Ohmura, W. H. Tuan, M. Naito. Rapid Thermal Conductivity Measurement of Porous Thermal Insulation Material by Laser Flash Method, Advanced Powder Technology 27 (2016) 882-885.

[3] T. W. Lian, A. Kondo, T. Kozawa, M. Akoshima, H. Abe, T. Ohmura, W. H. Tuan, M. Naito. Effect of Hydrophobic Nano-silica on the Thermal Insulation of Fibrous Silica Compacts, Journal of Asian Ceramic Societies 5 (2017) 118-122.

[4] T. Ohmura, T. W. Lian, A. Kondo, R. Hayasaka, M. Naito. Measurement Method of Thermal Conductivity in Ununiformed Temperature Field, Netsu Bussei 31 (2017) 166-173.

[5] T. W. Lian, A. Kondo, T. Kozawa, T. Ohmura, W. H. Tuan, M. Naito. Effect of Mechanical Processing on Thermal and Mechanical Properties of Fibrous Fumed Alumina Compacts, Journal of Asian Ceramic Societies, under submission.